

**Process planning for the subtractive rapid manufacturing of heterogeneous materials: Applications for automated bone implant manufacturing**

by

**Shuangyan Lei**

A dissertation submitted to the graduate faculty

In partial fulfillment of the requirements for the degree of

DOCTOR OF PHILOSOPHY

Major: Industrial Engineering

Program of Study Committee:  
Matthew Frank, Major Professor  
Frank Peters  
John Jackman  
Iris Rivero  
Eliot Winer

Iowa State University  
Ames, Iowa

2014

Copyright © Shuangyan Lei, 2014. All rights reserved

## TABLE OF CONTENTS

TABLE OF CONTENTS .....	ii
ABSTRACT .....	iv
CHAPTER 1. INTRODUCTION.....	1
1.1 Background.....	1
1.2 Motivation.....	9
1.3 Objective .....	11
1.4 Reference .....	12
CHAPTER 2. LITERATURE REVIEW.....	16
2.1 Heterogeneous Object Modeling and Manufacturing .....	16
2.2 Process Planning for Rapid Manufacturing .....	19
2.2.1 Fixture Design.....	19
2.2.2 Setup Orientation Determination .....	22
2.3 Process Planning for Rapid Manufacturing of Heterogeneous Materials .....	26
2.4 Reference .....	29
CHAPTER 3. A METHOD TO REPRESENT HETEROGENEOUS MATERIALS FOR RAPID PROTOTYPING – THE MATRYOSHKA APPROACH .....	38
Abstract.....	38
3.1 Background.....	39
3.2 The <i>Matryoshka</i> Shell Model.....	46
3.2.1 Using a Matryoshka Model for Bone Implant Harvesting .....	52
3.2.2 Creating a Discretized Slice Model .....	55
3.2.3 Density Score and Similarity Score Calculation .....	57
3.3 Implementation Example .....	60
3.3.1 Matryoska Model Generation and Harvesting Search .....	60
3.3.2 Implant Harvesting Using CNC-RP .....	65
3.4 Conclusion .....	68
3.5 Reference .....	69
CHAPTER 4. AUTOMATED FIXTURE DESIGN FOR THE SUBTRACTIVE RAPID MACHINING OF HETEROGENEOUS MATERIALS: APPLICATIONS FOR NATURAL BONE IMPLANT MANUFACTURING .....	74
Abstract.....	74
4.1 Introduction .....	75
4.2 Related Work .....	81
4.3 Overview of Sacrificial Support Generation for a Bone Implant .....	83
4.4 Implementation Example .....	100
4.5 Conclusion .....	105
4.6 Reference .....	106

CHAPTER 5: CONCLUSION AND FUTURE WORK .....	110
5.1 Summary .....	110
5.2 Future Work .....	113
5.2.1 Improving the Harvest Search Algorithm .....	113
5.2.2 Rotation Axis Selection.....	114
ACKNOWLEDGEMENTS .....	118

## ABSTRACT

This research presents a subtractive rapid manufacturing process for heterogeneous materials, in particular for custom shaped bone implants. Natural bone implants are widely used in the treatment of severe fractures or in tumor removal. In order for the human body to accept the bone implant material and heal properly, it is essential that the bone implant should be both mechanically and biologically compatible. Currently, the challenge of having correctly shaped natural bone implants created from an appropriate material is met through hand-shaping done by a surgeon.

CNC-RP is a rapid machining method and software that can realize a fully automated Subtractive Rapid Prototyping (RP) process, using a 3-axis milling machine with a 4<sup>th</sup> axis indexer for multiple setup orientations. It is capable of creating accurate bone implants from different clinically relevant material including natural bone. However, there are major challenges that need to be overcome in order to implement automated shape machining of natural bones. They are summarized as follows:

(1) Unlike homogeneous source materials for which a part can be machined from any arbitrary location within the original stock, for the case of donor bones, the site and orientation of implant harvest need to consider the nature of the heterogeneous internal bony architecture.

(2) For the engineered materials, the source machining stock is in the convenient form of geometrically regular shapes such as cylinders or rectangular blocks and the entities of sacrificial supports can connect the part to the remaining stock material. However,

irregularly-shaped bones and the heterogeneity of bone make the design of a fixture system for machining much more complicated.

In this dissertation, two major areas of research are presented to overcome these challenges and enable automated process planning for a new rapid manufacturing technique for natural bone implants.

Firstly, a new method for representing heterogeneous materials using nested STL shells is proposed. The nested shells model is called the *Matryoshka* mode, based in particular on the density distribution of human bone. The *Matryoshka* model is generated via an iterative process of thresholding the Hounsfield Unit (HU) data from a computed tomography (CT) scan, thereby delineating regions of progressively increasing bone density. Then a harvesting algorithm is developed to determine a suitable location to generate the bone implant from within the donor bone is presented. In this harvesting algorithm, a density score and similarity score are calculated to evaluate the overall effectiveness of that harvest site.

In the second research area, an automated fixturing system is proposed for securing the bone implant during the machining process. The proposed method uses a variant of sacrificial supports (stainless surgical screws) to drill into appropriate locations and orientations through the free-form shaped donor bone, terminating at proper locations inside the solid part model of the implant. This automated fixturing system has been applied to machine several bone implants from surrogate bones to 3D printed *Matryoshka* models. Finally, the algorithms that are developed for setup planning are

implemented in a CAD/CAM software add-on called “CNC-RP<sub>bio</sub>”. The results of this research could lead to a clinically relevant rapid machining process for custom shaped bone implants, which could create unique implants at the touch of a button. The implication of such high accuracy implants is that patients could benefit from more accurate reconstructions of trauma sites, with better fixation stability; leading to potentially shorter surgeries, less revisions, shorter recovery times and less likelihood of post-traumatic osteoarthritis, to name a few.

## CHAPTER 1. INTRODUCTION

With recent advancements in the rapid manufacturing technology, complex parts with varying material properties can now be created effectively. This research focuses on developing process planning algorithms for subtractive rapid manufacturing of parts with heterogeneous materials, in particular, developing rapid manufacturing methods to create custom bone implants from donated human bones. This chapter presents challenges in process planning for this system, followed by the motivation and objective of this research.

### 1.1 Background

Rapid Prototyping (RP), also known as layer based manufacturing, generally refers to techniques that can create 3D parts by the process of successively adding 2D layers of material [1]. The generic idea of “RP” has been more recently garnering the name “Additive Manufacturing” owing to the method of construction and the increasing functional use of the components created. This manufacturing approach takes complicated 3D geometry and slices it into simple 2D entities, which can be easily created through simpler fabrication processes. Most existing “RP” techniques are additive in nature, some are hybrid combinations of additive and subtractive methods, while some are purely subtractive. Commercial additive RP technologies include methods such as Fused Deposition Modeling (FDM), Stereolithography (SLA), Three Dimensional Printing (3DP), Laser Engineered Net Shaping (LENS), Selective Laser Melting (SLM), etc. [2-5]. In particular, the multi-material 3D printing system Connex

developed by Object Ltd. has the capability of printing parts made of up to fourteen different materials in a single print.

However, Additive Manufacturing is limited in the variety of materials available and geometric accuracy possible. The geometry error is usually caused by the stair-case effect of adding material layer by layer. Though a wide range of homogeneous and heterogeneous material mixtures have been employed in additive manufacturing, there is still a need for developing additional materials [6, 7]. Moreover, many of the materials which are commonly used in additive RP manufacturing processes cannot be used directly for fabricating functional models, especially dimensional tolerances or surface finishes when the part is required to be made from metal [8].

In order to improve the variety of materials available, subtractive rapid manufacturing has been developed in an effort to produce functional prototypes using appropriate materials. It can be used to rapidly machine a variety of functional parts with high accuracy and relatively low cost [9-11]. CNC-RP is a version of subtractive RP that can create functional 3D parts from a wide variety of materials [12-17]. It provides completely automated process planning, from initial setup planning through NC code generation. In this system, the stock material is fixed between two opposing chucks and is oriented by a rotary device. For each orientation, all visible surfaces of the part are machined to create part geometry. During the machining process, sacrificial supports are implemented as small features added to the part model geometry and incrementally created during the machining process along with other part features. At the end of the machining process, the supports are left to connect the part and stock material and then

the supports are subsequently cut to remove the part. Figure 1 illustrates the process steps for creating a part in CNC-RP. The cylindrical stock is shown fixed between opposing chucks in Figure 1(a). Four supports are used as shown in Figure 1(b), and 4 orientations are needed to machine the part and supports as shown in Figure 1(b.1-b.4). By the end of machining process, only permanent supports are remaining to provide stiffness to the part (Figure 1(b.5)). Lastly, the part is cut from the stock by sawing the two remaining supports (Figure 1(b.6)).

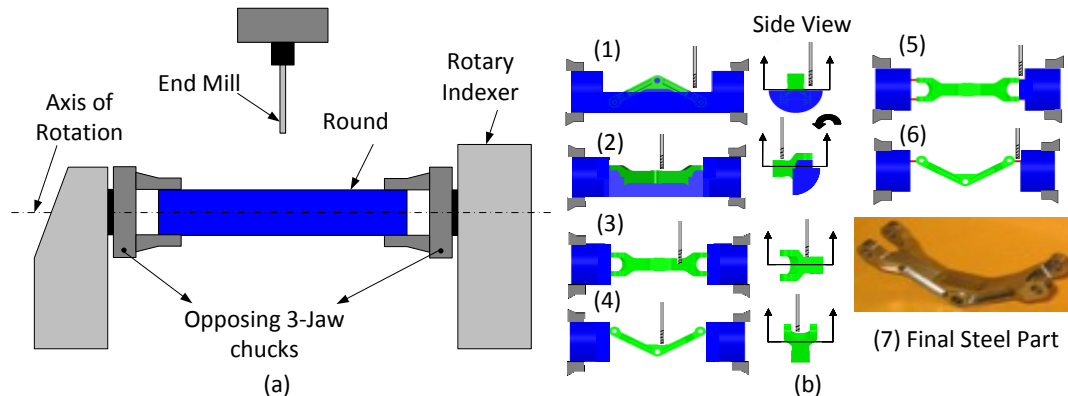


Figure 1. CNC-RP process (a) Rotary fixture setup; (b) Process sequence of steps (b.1 - b.4) to expose component geometry and (b.5 - b.6) to expose sacrificial supports.

In the current CNC-RP process, the source material usually has a regular shape, such as a cylindrical or rectangular bar and the part can be machined from anywhere arbitrarily within the original stock. However, challenges exist when manufacturing parts with multi-material or heterogeneous materials, in particular, since both the part and stock material could have an arbitrary shape and/or arbitrary heterogeneous material structure. As opposed to homogenous material from round bar, one would now need to determine a proper site from within the stock where the part can be feasibly machined.

One particularly challenging heterogeneous material is natural bone. Native human bone's density distribution from inside to outside spans a significant range. To illustrate, Figure 2 shows a cross sectional view of a femur bone, showing the spongy, low density trabecular bone in the middle, versus the high-density cortical bone on the outside.

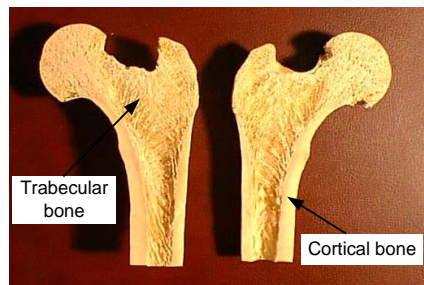


Figure 2. A Cross-sectional view of a femur bone [18].

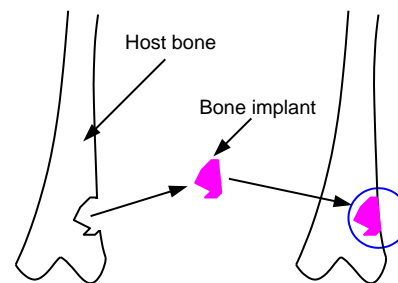


Figure 3. Typical bone implant (pink).

Bone implants are widely used in the treatment of missing pieces of bone due to trauma or other cases of bone loss (Figure 3). An estimated 15.3 million fractures occur annually in the United States, with some requiring significant bone reconstruction, requiring a burdensome task to perform the implant creation [19]. At the same time, the aging populations of the world and the increasing incidence of osteoporosis indicate that the repair of bone defects and fractures will be a major challenge for orthopedic surgeons [20]. Currently, persons over 65 years account for 12% to 13% of the total population; by 2030 it is expected this number will increase to 20%, an increase of more than 50% [19]. These people are at great risk of bone defects caused by osteoporotic fracture (80% of fractures in women over 60 years old [21]), infections, or cancer metastases. The treatment of bone defects that cannot self-repair may then become a

public health issue, resulting in a significant cost to society. The estimated cost for treatment of patients with musculoskeletal conditions in the USA already reached \$510 billion a decade ago in 2004 [19].

Bone grafting is a surgical procedure that places new bone into spaces between or around fractured bone to aid in healing. Bone grafting is possible because the bone possesses the capacity for regeneration as part of the repair process in response to injury. The application of the bone graft can be traced back to 1821, where the first clinical autograft was performed in Germany in an attempt to fill an animal skull defect. In 1879, Sir William Macewen successfully used a bone graft from other patients to reconstruct a 4 year old boy's proximal humerus, which is considered to be the first documented allograft procedure [22, 23].

Autologous bone grafting involves utilizing bone obtained from a healthy area of the patient's skeleton itself. It is the gold standard for augmentation of bone healing. It is known to be completely tissue compatible, and has no risk for disease transmission. Clinically, autologous bone grafting is commonly used in the treatment of fracture non-unions [24-27]. When a fracture fails to heal, it can result in non-unions. While non-unions can occur in any bone, they are most common in the tibia, humers, talus, and fifth metatarsal bone. However, failure rates have been reported to be as high as 50%, and this could be caused by different types of harvesting, handling, and/or the implementation method used and differences between patient conditions [28]. Autologous bone grafting has some significant drawbacks. Firstly, an additional surgical site is required, resulting in adding another potential location for postoperative pain and

complications, morbidity and infection. Secondly, the limited amount of available graft is another drawback.

In the absence of autologous bone for harvesting, fresh-frozen allograft bone was developed as a viable alternative. During the last two decades, the use of fresh-frozen allograft bone has significantly increased [29-32]. Allograft bone, like autologous bone, is derived from humans but not the patient's skeleton itself; it is obtained from a donor. In general, allograft bone is taken from donated cadavers at a bone tissue bank. One common concern with using allograft bones is the possibility of viral disease transmission. However, strict measures are applied to ensure safety of the transplanted tissue. Similarly, strict guidelines have been established for bone processing, which define the donor bone selection process, how the bone must be harvested, processed and stored, together with thorough record-keeping procedures [33]. That all being said, there does remain the risk of infection, disease transmission or an immune response [34].

These drawbacks led to the development of new strategies for repairing bone defects, including the use of bone graft substitutes as alternatives to autologous or allograft bone grafts. Bone graft substitutes consist of scaffolds made of synthetic or natural biomaterials that are able to integrate with the host bone. There are a variety of bone graft substitutes that are being used clinically. Demineralized bone matrix (DBM) and collagen are biomaterials, used mainly as bone-graft extenders for filling bone defects and cavities. Ceramic-based synthetic bone graft substitutes, such as hydroxyapatite (HA),  $\beta$ -tricalcium phosphate ( $\beta$ -TCP) and are bioactive glass ceramics, which have

been used as adjuncts or alternatives to autologous bone grafts. Approximately 60% of the synthetic bone graft substitutes currently available involve ceramics [22]. Degradable synthetic polymers are bone graft substitutes that are resorbed by the body so after healing there remain no foreign bodies. It has been used as a stand-alone device and grafted with hyaluronic acid for periodontal barrier applications [35]. In addition, there are also non-biological substrates, such as fabricated biocompatible metals, (e.g., porous tantalum) that are compatible with the bone growth and stay strong and inert in the body. Research is ongoing to improve the mechanical properties and biocompatibility of scaffolds to promote bone repair [36].

Due to advancements in the field of biomaterials, many biocompatible materials like solid metal, porous metal, ceramics, plastics, composites, etc. have been successfully used in bone repair or joint replacements. As representative tests, similar materials have been evaluated for use in the CNC-RP process to show the flexibility of the method. Figure 4 provides a sample of several materials used to replicate a CT-derived section of bony anatomy from a fracture case.

Biomedical implant manufacturing using layer-based additive techniques has also made significant progress in fabricating patient-specific implants. These techniques include Selective Laser Melting (SLM), Stereolithography (SLA), Electron beam melting (EBM), Direct Metal Laser Sintering (DMLS), 3DP, LENS, etc. SLM was shown as a possible process to manufacture 3D porous metallic structures using a variety of material options, including stainless steel, titanium, and chromium-cobalt [37]. EBM technology has been relatively widely used to fabricate custom designed implants for knees, hips,

elbows, shoulders, fingers, and bone plates in titanium (Ti6A14V) [38,39]. LENS has also been used to make load bearing metal porous implants with complex anatomical shapes from materials like Ti, Ti6A14V, Ni-Ti and CoCrMo alloys. The surface porosities and load bearing properties of the manufactured implants depend on parameters like laser power, power feed rate and scan speed [40-42]. Apart from that, SLA can be used to create tissue geometry of arbitrary 3D shapes directly from CAD data. In addition, low-density cellular materials with gaseous voids have been manufactured by SLA technologies [43]. This cellular structure material makes the bone grow into implants for biological fixation, such as an acetabular implant with gradient porosity for hip replacements [44].

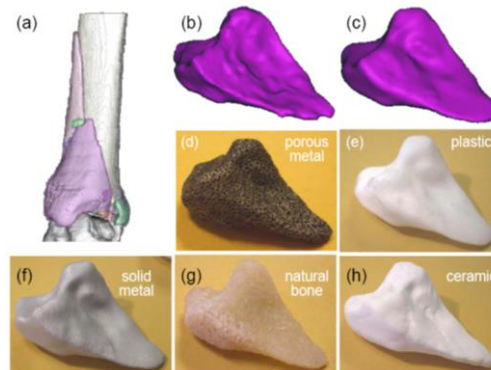


Figure 4. Images of fragments: (a) Comminuted fracture bed as directly segmented from patient CT data; (b) individual computational fragment image as extracted from the fracture bed, and (c) as computationally smoothed. Corresponding 3D fragment geometries subtractively rapid-manufactured from (d) Trabecular Metal<sup>®</sup> (e) Plastic, (f) solid metal, (g) bovine cortical bone, and (h) porous ceramic.

Although additive RP technologies provide the ability to create complex shapes in some biocompatible materials; other approved and desired materials are not usable, in particular, natural bone. Allograft bone often holds strong preferential attraction over artificial biocompatible materials in many situations clinically [45, 46]. However, challenges need to be overcome in order to implement automated shape-machining of allograft bone. Unlike for the homogeneous source material, the part can be machined from anywhere arbitrarily within the original stock. Since natural bone has a heterogeneous structure, the site and orientation of implant harvest needs to consider the internal bony architecture. Currently, the challenge of making natural bone implants is done through the hand-shaping by a surgeon.

To date, there has been little research involving harvesting implants from natural bone, at least not in rapid manufacturing research. This work presents a method for rapid manufacturing of custom bone implant from natural bone through CNC machining and solves some very fundamental problems that would enable its effective use.

## **1.2 Motivation**

Rapid manufacturing processes typically use a layer based manufacturing technique to create functional or small batches of parts directly from computer-aided design (CAD) models of the components. This not only shortens the pre-process engineering time, but also provides a “turn-key” solution to reduce human intervention in the process planning required for manufacturing. As a new approach, the CNC-RP process combines CNC

machining with RP methodologies in order to create functional parts in a completely automated fashion, directly from CAD.

The handcrafting of implant geometries specific to a patient can lead to some relative geometrical errors, making the bone implant less effective in the long term. Developing an approach to automated rapid manufacturing of natural bone implants is highly desirable; however, little research has been done in this field. There are some major challenges that need to be solved in order to implement automated shape machining of allograft bone using CNC-RP. They can be summarized as follows:

(1) The CNC-RP process uses a homogeneous source stock material, from which the part could be machined from anywhere arbitrarily within the original stock. In contrast, natural bone has a heterogeneous internal structure, hence the harvest site and orientation of the implant needs to consider the bone density profile.

(2) The stock used in CNC-RP is in the convenient form of geometrically regular shapes such as cylinders or rectangular blocks and the sacrificial supports simply connect the part to the remaining stock material. For allografts, the source stock material is restricted to irregularly-shaped donor bones and the heterogeneity of the bone structure makes the design of a fixture system for machining bone implant more complicated.

In this dissertation, we will present methodologies to solve the above challenges, and these methods are implemented in process planning software for the subtractive rapid manufacturing of heterogeneous materials.

### 1.3 Objective

The overarching objective of this research is to develop new process planning algorithms and software to realize the completely automatic process planning for a rapid machining system capable of handling heterogeneous materials of arbitrary geometry.

The first sub-objective is to propose a heterogeneous object modeling approach to represent heterogeneous materials for rapid prototyping, in particular, based on the density distribution of human bone. This model can characterize the heterogeneity of the bone structure. The goal of this new model is to enable a harvesting algorithm that can determine a suitable location for the bone implant from within a natural bone.

The second sub-objective is to design an automated fixturing system for subtractive rapid machining process of heterogeneous materials, based in particular on the bone implant. In traditional RP processes, the fixtures are called *sacrificial* support structures. In this research, the same idea of sacrificial support methodology is used to design the fixturing structures for the CNC machining of bone implants from intact bones.

Finally, the algorithms that were developed for process planning will be implemented in CAD/CAM software called "CNC-RP<sub>bio</sub>". The software can be used as an automatically process planning software to machine natural bone implant.

If successful this work will serve to enhance the array of methods to help people in society who have suffered greatly in traumatic injuries. Whether it is from a car accident, high-height fall, or an injury suffered in combat, this research will provide a new method

to enable natural bone implants to be effectively and efficiently produced, nearly at the push of a button. Automated of many of the steps will allow the method to tackle challenging trauma cases, making one-of-a-kind functional parts for anyone, without the exorbitant costs associated with custom manufacturing

#### 1.4 Reference

- [1] Yan, X. and Gu, P., A review of rapid prototyping technologies and systems, *Computer Aided Design*, 1996, 28(4), 307-318.
- [2] Liu,W and DuPont, J.N., Fabrication of functionally graded TiC/Ti compo- sites by Laser Engineered Net Shaping, *Scripta Materialia*, 2003,48(9), 1337–1342.
- [3] Mumtaz, K. A. and Hopkinson, N., Laser melting functionally graded composition of Waspaloy and Zirconia powders, *Journal of Materials Science*,2007,42(18), 7647–7656.
- [4] Jackson, T. R., Liu,H., Patrikalakis,N.M., Sachs, E.M. and Cima, M.J., Modeling and designing functionally graded material components for fabrication with local composition control, *Materials and Design*, 1999, 20(2-3), 63-75.
- [5] Dimitrov,D., Schreve,K. and Beer,N., Advances in three dimensional printing – state of the art and future perspectives, *Rapid Prototyping Journal*, 2006, 12(3),136–147.
- [6] Hague, R., Mansour, S. and Saleh, N., Material and design considerations for rapid manufacturing”, *International Journal of Production Research*, 2004, 42(22), 4691-4708.
- [7] Hao, L., New material development for laser additive manufacturing, *Proceedings of the 5th International Conference on Advanced Research in Virtual and Rapid Prototyping*, Leiria, Portugal, 2011,359-364.
- [8] Pham, D.T. and Gault, R.S., A comparison of rapid prototyping technologies, *International Journal of Machine Tools and Manufacture*, 1998, 38(10-11), 1257-1287.
- [9] Hassold, R., CNC machining as a rapid prototyping technique, *Modern Machine Shop*, 1995, 68(5), 68-73.
- [10] Schmidt, J. W., CNC machining - the other rapid prototyping technology. *In Proceddings of 1997 International Congress and Exposition*. 1997, 1233, 89-91.

- [11] Wang, F., Marchetti, L. and Wright, P. K., Rapid prototyping using machining, *Technical Paper - Society of Manufacturing Engineers*. 1999.
- [12] Frank, M.C., Wysk, R.A. and Joshi, S.B., Determining setup orientations from the visibility of slice geometry for rapid CNC machining, *Journal of Manufacturing Science and Engineering*, 2006,128(1), 228-238.
- [13] Li, Y. and Frank, M.C., Machinability analysis for 3-axis flat end milling, *Journal of Manufacturing Science and Engineering, Transactions of the ASME*, 2006, 128(2), 454-464.
- [14] Li, Y. and Frank, M.C., Computing non-visibility of convex polygonal facets on the surface of a polyhedral CAD model, *Computer-Aided Design*, 2007, 39(9), 732-744.
- [15] Frank, M.C. Implementing rapid prototyping using CNC machining (CNC-RP) through a CAD/CAM interface, Proceedings of the Solid Freeform Fabrication Symposium, 2007, 112-123.
- [16] Boonsuk, W. and Frank, M.C, Automated fixture design for a rapid machining process, *Rapid Prototyping Journal*, 2009, 15(2), 111-125.
- [17] Petrzela, E.J. and Frank, M.C., Advanced process planning for subtractive rapid prototyping, *Rapid Prototyping Journal*, 2010, 16(3), 216-224.
- [18]<http://academic.uofs.edu/faculty/kosmahle1/courses/pt245/trabecul.htm> (accessed October 20<sup>th</sup> 2012).
- [19] <http://www.boneandjointburden.org/about/>, The burden of musculoskeletal diseases in the United States, (accessed 1<sup>st</sup> 2014).
- [20] Lauzon, M.A., Bergeron, E., Marcos, B. and Fauchoux, N., Bone repair: New developments in growth factor delivery systems and their mathematical modeling, *Journal of Controlled Release*, 2012, 162(3), 503-520.
- [21] D. Garriguet, Bone health: osteoporosis, calcium and vitamin D, *Health Rep*, 2011, 22(3), 7-14.
- [22] Karachalios, T. Bone-Implant Interface in Orthopedic Surgery Basic Science to Clinical Applications, 2014.
- [23] Boer H.H., The history of bone grafts, *Clin Orthop Relat Res*, 1998, 226, 292-298.
- [24] Perry C.R., Bone repair techniques, bone graft, and bone graft substitutes, *Clin Orthop Relat Res*, 1999, 360, 71-86.

- [25] Lane J.M. Tomin, E. and Bostrom, M.P., Biosynthetic bone grafting, *Clin Orthop Relat Res*, 1999, 367, S107-S117.
- [26] Liu, G., Zhao, L., Zhang, W., Cui, L., Liu, W. and Cao, Y., Repair of goat tibial defects with bone marrow stromal cells and beta-tricalcium phosphate, *J Mater Sci Mater Med*, 2008, 19(6), 2367–2376.
- [27] Blokhuis, T.J., Wippermann, B.W., Boer, F.C., Lingen, A., Patka, P., Bakker, F.C. and Haarman, H.J., Resorbable calcium phosphate particles as a carrier material for bone marrow in an ovine segmental defect, *J Biomed Mater Res*, 2000, 51(3), 369-375.
- [28] Kanakaris, N.K., Paliobeis, C., Nianidakis, N. and Giannoudis, P.V., Biological enhancement of tibial diaphyseal aseptic non-unions: the efficacy of autologous bone grafting, BMPs and reaming by-products, *Injury*, 2007, 38(S2), S65-S75.
- [29] Bauer, T.W. and Muschler, G.F., Bone graft materials. An overview of the basic science. *Clin Orthop Relat Res*, 2000, 371, 10-27.
- [30] Schreurs, B.W., Slooff, T.J., Buma, P. and Verdonschot, N., Basic science of bone impaction grafting, *Instr Course Lect*, 2001, 50, 211-220.
- [31] Theler, J.M., Bone tissue substitutes and replacements, *Curr Opin Otolaryngol Head Neck Surg*, 2011, 19(4), 317-322.
- [32] Lavernia, C.J., Malinin, T.I., Temple, H.T. and Moreyra, C.E., Bone and tissue allograft use by orthopaedic surgeons, *J Arthroplasty*, 2004, 19(4), 430-435.
- [33] Spin-Neto, R., Landazuri Del Barrio, R.A., Pereira, L.A., Marcantonio, R.A., Marcantonio, E. and Marcantonio, E.J. Clinical similarities and histological diversity comparing fresh frozen onlay bone blocks allografts and autografts in human maxillary reconstruction, *Clin Implant Dent Relat Res*, 2013, 15(4), 490-497.
- [34] Giannoudis, P.V., Dinopoulos, H. and Tsiridis, E., Bone substitutes: an update, *Injury*, 2005, 36(S3), S20-S27.
- [35] Nandi, S.K., Roy, S. Mukherjee, P. Kundu, B., De, D.K. and Basu, D., Orthopaedic applications of bone graft & graft substitutes: a review, *Indian J Med Res*, 2010, 132(1), 15-30.
- [36] Zwingenberger, S. Nich, C., Valladares, R.D., Yao, Z., Stiehler, M. and Goodman, S.B. Recommendations and considerations for the use of biologics in orthopedic surgery, *BioDrugs*, 2012, 26(4), 245-256.

- [37] Kruth, J.P., Mercelis, P., Vaerenbergh, J.V., Froyen, L. and Rombouts, M., Binding mechanisms in selective laser sintering and selective laser melting, *Rapid Prototyping Journal*, 2005, 11(1), 26-36.
- [38] Harrysson, O.L.A., CansiZoglu, O., Marcellin-Little, D.J., Cormier, D.R. and West, H.A., Direct metal fabrication of titanium implants with tailored materials and mechanical properties using electron beam melting technology. *Materials Science & Engineering.C, Biomimetic Materials, Sensors and Systems*, 2008, 28(3), 366-373.
- [39] Thomsen, P., Malmström, J., Emanuelsson, L., René, M. and Snis, A., Electron beam-melted, free-form-fabricated titanium alloy implants: material surface characterization and early bone response in rabbits, *Journal of Biomedical Materials Research Part B Applied Biomaterials*, 2009, 90(1), 35-44.
- [40] España, F.A., Balla, V.K., Bose, S. and Bandyopadhyay, A., Design and fabrication of CoCrMo alloy based novel structures for load bearing implants using laser engineered net shaping, *Materials Science and Engineering: C*, 2010, 30(1), 50-57.
- [41] Bandyopadhyay, A., Krishna, B.V., Xue, W. and Bose, S., Application of Laser Engineered Net Shaping (LENS) to manufacture porous and functionally graded structures for load bearing implants, *J Mater Sci Mater Med*, 2009, 20(S1), S29-S34.
- [42] Balla, V.K., Bodhak, S., Bose, S. and Bandyopadhyay, A., Porous tantalum structures for bone Implants: fabrication, mechanical and in vitro biological properties, *Acta Biomater*, 2010, 6(8), 3349-3359.
- [43] Williams, C.B., Mistree, F.M. and Rosen, D.W., Investigation of solid freeform fabrication processes for the manufacture of parts with designed mesostructure. ASME IDETC Design for Manufacturing and the Life Cycle Conference, 2005.
- [44] Wang, H., Johnston, S.R. and Rosen, D.W., Design of a graded cellular structure for an acetabular hip replacement component, The Seventeenth Solid Freeform Fabrication Symposium, 2006, 111-123.
- [45] Skendzel J.G. and Sekiya J.K., Arthroscopic glenoid osteochondral allograft reconstruction without subscapularis takedown: technique and literature review, *Arthroscopy*, 2011, 27(1), 129-135.
- [46] Clowers B.E. and Myerson M.S., A novel surgical technique for the management of massive osseous defects in the hindfoot with bulk allograft, *Foot Ankle Clin*, 2011, 16(1), 181-189.

## CHAPTER 2. LITERATURE REVIEW

In this chapter, related research in the fields of heterogeneous object modeling, process planning for rapid manufacturing, and process planning for manufacturing heterogeneous materials are reviewed.

### 2.1 Heterogeneous Object Modeling and Manufacturing

Heterogeneous materials, in general, refer to objects with spatially different material compositions or structures [1, 2]. Heterogeneous objects are mainly classified into two groups, multi-material objects, which have distinct material domains and functionally graded materials (FGMs), which have continuous material variation in composition and structure gradually over volume.

In the past few decades, heterogeneous objects have gained more research interest and extensive work has been undertaken in heterogeneous object modeling. The existing models investigating this topic fall into two categories, evaluated models and unevaluated models, depending on the representational exactness and compactness [3]. Evaluated models are inexact and represent heterogeneous materials distribution through intensity space decompositions. Typical models are voxel models [4, 5] and volume mesh based models [6]. Unevaluated models utilize exact geometric data representation and rigorous functions to represent the material distributions, such as explicit functional representations [7-9], control feature based models [10-13], control point based models [14], and implicit function based models [15].

A variety of heterogeneous object modeling methods have been presented in the literature. However, some challenges remain with how we represent the complex models that RP systems can manufacture. This includes not only multi-material models, but for other complex geometries in general. For example, additive RP machines can create complex scaffolds, but we are still developing new methods to easily represent models such as bone scaffolds, biomimetic objects, or other complex natural structures with computational efficiency. Bibb and Sias used the SLA technique to build cancellous bone structure models and investigated the problems associated with the CAD model which is saved in STK and SLC file format [15]. Chen et al. put forward a technique to fabricate the mold of an artificial bone composed of a nontoxic soluble material by using two CAD models [16]. The external contour CAD model and the internal microtubule structure CAD model. The external contour model is obtained by reconstructing the 3D geometry from bone computed tomography (CT) scanning data and saved into STL format. The internal microtubule structure model is built up through micrographs and histological analysis. Sun et al. presented a method to develop a femur model by using quantitative computed tomography number (QCTN) to characterize the bone mechanical properties [17]. It used different QCTN to characterize the density of the tissue in different layers and considered both cancellous and cortical bone smeared together as one structure in each layer. Fang et al., proposed a multi-scale voxel modeling approach to model the bone structure at the macroscopic and microscopic level and developed a Direct Fabrication (DF) system to fabricate a tissue scaffold constructed with random heterogeneous microstructure and designed shape [18].

Due to the developments in the manufacturing technologies (e.g. layered manufacturing) and applications (e.g. functionally graded material), heterogeneous materials manufacturing has gained more attention. An example is a heterogeneous pressure vessel [19], where the material on the inner surface of the pressure vessel is ceramic which has good high temperature properties and the material on the outside is metal which has good mechanical properties. In order to join the two materials, the composition of the metal needs to be gradually increased in a controlled manner, starting from zero at the inner surface to unity at the outer surface. The Shape Deposition Manufacturing (SDM) process at Stanford presented the possibility of creating metallic artifacts with functional gradient materials [20]. It used laser deposition to fuse metallic powders onto a substrate and these powders could be mixed to create a range of alloys. Laser-assisted micro-SDM [21] was a variation of SDM, which aimed at fabricating 3D heterogeneous micro-components. Wang et. al. [22] developed a hybrid manufacturing technology, which involved layered manufacturing, micro-fabrication and mechanical machining to fabricate components made of a multiphase material. In the 3DP system, powder particles are bonded together with a binder or solvent for the powder, which is delivered via an inkjet print head [23]. The 3DP process has been applied to build parts derived from metal and ceramic powders [24, 25]. Direct Metal Deposition (DMD) technology [26, 27], developed at the University of Michigan, was a laser aided rapid manufacturing technology which can be used to fabrication porous or solid metallic parts directly and had the capability to fabricate heterogeneous objects [28]. Similar to DMD, the Laser Engineering Net Shaping (LENS)[29,30] process developed at Sandia National Laboratories is a system which has been used to deposit

a broad range of materials, including stainless steel, nickel-based superalloys, copper alloys, and titanium alloys with enhanced physical and mechanical property. It has also been demonstrated to have the capability of manufacturing 3D heterogeneous objects [31]. Selective Laser Sintering (SLS) [32, 33] uses a high power laser to fuse powder and has been applied to produce heterogeneous objects [34, 35].

## **2.2 Process Planning for Rapid Manufacturing**

In the manufacturing process chain, an essential task is the preparation for the fabrication steps, which is generically referred to as *process planning*. In the simplified methods of additive manufacturing, process planning is usually limited to orientation planning and support structure design, but can include some other details depending on the specific materials or process.

### **2.2.1 Fixture Design**

Fixture design techniques involve providing proper part orientation, location, supports, and clamping such that all the model features can be created. Traditional fixturing techniques for machining use hardware such as clamps, vises, V-block, modular plates, etc. This introduces several disadvantages such as clamping induced error, reduced workability for tools and increased process planning complexity and setup time. Therefore, an innovation to fixturing and fixture design could result in significant improvement of the accuracy of machined parts and the time from CAD to part. As a result, a great deal of attention has been directed towards the development of flexible fixture systems in the past decades [36, 37].

In some current additive RP processes, the fixtures used to hold the part are called *sacrificial support structures*, which are automatically added during the building process. The sacrificial support structure is intended for temporarily supporting the overhanging features of the part and then to be eliminated in the post-processing step. In general, sacrificial support is divided into two basic categories: *passive* sacrificial supports and *active* sacrificial supports. In a passive support system, the support is a result of the processing method; not a specifically design scaffolding that is built in process. Passive sacrificial supports are used in SLS and 3DP, since the part being constructed is surrounded by un-sintered/un-fused powder at all times [38, 39]. In Contrast, a variety of research has investigated the design of active sacrificial support structure, particularly in the development of Stereolithography (SLA) and Fused Deposition Modeling (FDM) [41-43]. The automated support generation approach for mask image projection based additive manufacturing also provided a scientific foundation for generating *just* sufficient supports for arbitrary geometries [44]. Currently, this method has been incorporated by EnvisionTec in its Perfactory RP software system [45].

However, parts produced by additive manufacturing exhibits a stair-step surface effect due to the presence of 2-1/2 dimensional layers; which can limit the accuracy of the components. Several research efforts have focused on the surface roughness of various additive processes [46-48]. Another limitation can be the choices of materials available for an additive manufacturing system. The most common commercially available materials include photopolymers, plastics, or rubber and are mainly for the application of concept models, visual prototypes, and limited functional prototypes.

There are several metal AM machines available, but the processing cost is relatively high and they usually require post processing, which include machining. Subtractive RP manufacturing has been developed to overcome some of the above-mentioned limitations. There has also been considerable research to address fixture designs in conjunction with layer slicing and planning. Ajay and Joneja [49] developed an integrated software system called the Quick Turnaround Cell (QTC) for rapid prototyping. This fixture system is capable of machining prismatic parts but does not provide a feasible fixture solution for arbitrary part shapes. Tseng proposed [50] a feature-based fixturing analysis method to analyze the fixturing parameters required for the intermediate steps in a successive feature-based machining process. The output of the fixturing parameters includes locating faces, location points, clamping points and feasible height ranges for locating and clamping devices. However, the shape of parts was restricted to prismatic parts and prismatic features, once again. Gandhi et al. [51, 52] proposed a fluidized bed technique as a flexible fixturing process. It utilizes materials that can change from a solid phase to a liquid phase and vice versa. When the material is in the liquid state, the fixturing medium can accommodate a wide variety of different part geometries, while in the solid state the part is held fixed. Similarly, Choi et al. developed the Reference-Free Part Encapsulation (RFPE) system, which could fixture arbitrary geometric shapes during a machining process [53]. The basic concept involved filling the space with low melting point matter for holding. After all the machining had been completed, the filler material was finally melted away. Shin et al. proposed a new type of technology using a combination of high-speed machining technology and an automatic fixturing process [54]. It used low-melting-point metal

alloys to hold the workpiece during multi-face machining. However, a considerable amount of time is required for the workpiece fixturing process. DeskProto [55] uses a rotary axis and support tabs to hold the part during the machining, however, it does not provide analysis about the support design to determine if it is a feasible solution for any arbitrary part. Roland [56] uses a similar fixture approach, with support tabs that are added to the part, but it does not give an optimized or validated design to show the supports work for any free-form parts. Boonsuk and Frank developed an automated fixture design for a rapid machining process [57], which includes the design of sacrificial support length, shape, size, number, and location to maximum allowable deflection of the part while maximizing machinable surface area. However, in this sacrificial design, it considers the part is made of one homogeneous material.

Although this is considerable amounts of related work, there is no effective automated fixturing system to create a model in a subtractive rapid manufacturing process with heterogeneous materials in the literature.

### **2.2.2 Setup Orientation Determination**

In an additive RP process, the setup orientation determines the building direction of the part (typically along the 'z' axis, or vertical direction). Various factors can be considered in the part orientation selection process. These factors could be the total building time, quality of part surfaces, amount of the support structure used during the fabrication, or complexity of the support structure [58-59].

The determination of a proper orientation of the part during the building process has been a subject of research in additive RP for decades. Cheng et al. proposed a multiple objective approach to determine the optimal part orientation applying building time and part accuracy as objectives for SLA process [60]. The first primary objective is the part accuracy, which is calculated based on experience for different types of surface. And the second primary objective is the minimum building time that is achieved by reducing the number of slices. Hur and Lee developed an algorithm to calculate the staircase area, quantifying the process errors by the volume supposed to be removed or added to the part, and the optimum layer thickness for the SLA system [61]. The part accuracy, the total building time, and the volume of the support structures were the factors considered. The optimal part orientation is determined based on the user's selections of primary criteria and the optimal thickness of the layers. Byun and Lee proposed a generic algorithm which aimed to determine the optimal part orientation that improved the average weighted surface roughness generated from the stair stepping effect and also minimized the building time including the structure of the support in fabrication a completely freeform part for the FDM process [62]. In SLS process, where no active supports are necessary, changes in part quality are primarily due to building time, part strength, and rough surfaces due to the rasterization of facets at angles to the building direction. Thompson and Richard determined the building orientation for SLS based on the consideration of optimizing part quality [63]. Padhye and Kalyanmoy proposed a multi-objective optimization approach to find the optimal build orientations in an SLS process by considering minimization of surface roughness and build time [64]. Alexander et al. presented a method to choose suitable part orientation for better

accuracy and lower cost [65]. In their approach, a generic model is used to calculate the total cost of a model which includes pre-build, build, and post-processing costs. Mosood et al. described a volumetric error based approach to determine suitable part build orientation for an FDM process [66, 67]. The methodology involved a primitive volume approach, which assumed that a complex part is to be constructed from a combination of basic primitive volumes. The optimal part orientation is determined when the part has the minimum volumetric error. The methodology has been shown to work for various primitive volumes and for simple parts made from cylinders, cubes, spheres and pyramids. Lin et al. presented a mathematical model to predict the layered process error and proposed an optimization algorithm to define the orientation based on minimum process error [68]. Case studies have been implemented to determine the preferred orientation for fabricating spheres, cubes and some freeform shapes.

In the subtractive RP process, the selection of an axis of rotation is a critical step in process planning, since a proper axis of rotation provides tool accessibility, reducing the number of setups and could eliminate the need for re-fixturing. A suitable set of setup orientations about a rotary indexer can make it feasible to machine the entire part surface completely. The research on this issue can be classified into two categories, whether they use feature recognition or not. In the past, feature based technologies have been an active field among the manufacturing research community and feature recognition has been applied to matching setup planning. Hebbal and Mehta developed an approach to select an optimal setup plan for machining the features of a given prismatic part [69]. The proposed setup planning from both machining and fixturing

viewpoints generally consisted of: (1) identifying groups of features that can be machined in a single setup, (2) determining a suitable work piece orientation, i.e. the suitable datum planes for each setup, (3) determining all the feasible setup plans to machine the given set of features of prismatic parts, and (4) evaluating the feasible setup plans on the basis of tolerance and total setup time. Ferreira and Liu described a rule-based system to generate good orientations, with each orientation corresponding to a setup [70]. Ong et al. presented a concurrent constraint planning methodology for setup planning and re-set-up planning in a dynamic workshop environment [71]. Ong and Chew proposed a manufacturability and setup evaluation methodology which used fuzzy set theory and an analytical hierarchy process method to evaluate the accessibility, orientation, dimensional tolerance, and surface finish specifications of a part [72]. Boerma et al developed an approach to use the tolerance specifications for setup and fixture selection [73]. In this approach, the selection of setups depended on: (1) the accuracy of the relations between the features, (2) the approach directions of the features involved and (3) the number and directions of the machine tool axes. In this work, fuzzy-set theory was also applied to set-up planning [74-77].

However, in many cases, free-form shapes may not have definable “features”, which makes feature-based set-up planning approaches largely incapable. Gan et al. and Suh et al. constructed a visibility map for a Gaussian map, which is useful for computation of surface-surface intersection, component design for manufacturing, machinability analysis, etc [78, 79]. In [80, 81], the researchers used a visibility map constructed from a Gaussian map to computer setup orientations for four- and five- axis machining and

an efficient “greedy” approach is presented to find a workpiece orientation that allows the maximum number of surfaces to be machined in a single setup. Then a second such orientation is found for the un-machined surfaces, and so on. Radzevich and Goodman also used the concept of a Gaussian image in the context of finding an optimal workpiece orientation in multi-axis NC machining [82]. Their methodology takes into account the geometry of the part surface to be machining, the machining surface of the tool, and the degrees of freedom available on multi-axis NC machining. Gupta et al. proposed an efficient geometric algorithm for orienting a workpiece on 4 and 5 axes NC machines to maximize the number of part faces that can be machined in a single setup [83]. The algorithm is based on geometric duality, topological sweep, intersection and covering on the unit-sphere, and techniques for efficiently constructing and searching an arrangement of polygons on the unit-sphere. Li and Frank presented a feature-free method for determining feasible axes of rotation for setup planning, based on the visibility of a polyhedral model [84]. The visibility map can provide a quantitative evaluation of a surface, a feature or an entire part model.

### **2.3 Process Planning for Rapid Manufacturing of Heterogeneous Materials**

Additive manufacturing techniques, such as DMD [85, 86], shape deposition manufacturing (SDM) [87, 88], LENS [89], directed light fabrication (DLF) [90], and 3DP [91] have shown the capability to manufacture 3D heterogeneous objects. Currently, the process planning tasks involve selecting an orientation, creating supports, slicing and finally defining the fill pattern for each layer. These tasks, however, are mainly based on geometry and do not consider the effect of material variation in an object [92]. The

manufacturing of heterogeneous materials needs to selectively deposit various materials throughout an object, which is included as additional steps to incorporate the process planning of heterogeneous object fabrication. However, heterogeneous object fabrication capability is not widespread in current AM systems. Shin et al. [92] introduced a new process planning method that takes into account the processing of material information. The detailed tasks are pre-processing (discretization), orientation (build direction), and adaptive slicing of heterogeneous objects. This approach used a pre-processing step by which a heterogeneous object is discretized into a multi-material model that consists of mixed lumps of homogeneous material. An optimal build direction is chosen by approximately estimating build time, and the discretization process also allows adaptive slicing of heterogeneous objects to minimize surface finish and material composition error. In [93, 94], a novel approach of representation and process planning of FGMs, termed as equal distance offset (EDO), was developed. In EDO, a neutral arbitrary 3D CAD model is adaptively sliced into a series of 2D layers. Within each layer, 2D material gradients are designed and represented via dividing the 2D shape into several sub-regions enclosed by iso-composition boundaries, which is then followed by applying the EDO algorithm to each sub-region. This approach could be applied to arbitrary-shaped objects with 3D material composition gradients. Brad et al [95] presented a process planning method and control system for functionally graded material fabrication using a triple extruder Freeze-form Extrusion Fabrication (FEF) system including motion code generation, extruder dynamic modeling and control, and composition gradient control. A process planning algorithm was developed to integrate heterogeneous materials composition gradient information with the pre-processed tool

path from either insight or manually written NC code. A multi-material stereolithography (MMSL) system was introduced to stack different photo curable resins to produce a multiple-material part [96]. However, a core challenge in the use of multiple materials in SLA is how to manage material contamination between changing different materials used in the fabrication process. Kim et al. presented a process planning approach to minimize material changeover for a given multi-material CAD model [97, 98]. Zhou et al. introduced a multi-material mask-image-projection-based Stereolithography process to fabricate 3D components with spatially controlled digital material [99]. A multi-material virtual prototyping system for digital fabrication of heterogeneous prototypes was proposed by Chio and Cheung [100]. This system consisted mainly of a topological hierarchy-sorting algorithm for processing slice contours, and a virtual simulation system for visualization and optimization of multi-material layered manufacturing. The process planning included multi-tool path planning, build time estimation and accuracy analysis, integrated with semi- and full-immersive virtual reality technology [101]. Chen et al. introduced a virtual manufacturing system for components made of multiphase materials [102]. The software developed in this virtual system consisted of three sub-systems: one for process planning, one for numerical control (NC) coding, and one for quality assessment. The process planning involved the selection of a build orientation, fabrication sequence, 2D geometric boundaries, material information and a manufacturing process.

## 2.4 Reference

- [1] Sun, W., Multi-volume CAD modeling for heterogeneous object design and fabrication, *Journal of Computer Science and Technology*, 2000, 15(1), 27-36.
- [2] Chen, K. Z. and Feng, X. A., CAD modeling for the components made of multi heterogeneous materials and smart materials, *Computer-Aided Design*, 2004, 36(1), 51-63.
- [3] Kou, X.Y. and Tan, S.T., Heterogeneous object modeling: A review, *Computer-Aided Design*, 2007, 39(4), 284-301.
- [4] Chen, M. and Tucker, J.V., Constructive volume geometry, *Computer Graphics Forum*, 2000, 19(4), 281-293.
- [5] Chandru, V., Manohar, S. and Prakash, C.E., Voxel-based modeling for layered manufacturing, *Computer Graphics and Applications, IEEE*, 1999, 15(6), 42-47.
- [6] Jackson, T., Analysis of functionally graded material object representation methods, Ph.D. Dissertation, Massachusetts Institute of Technology, 2000.
- [7] Shin, K.H. and Dutta, D., Constructive representation of heterogeneous objects, *Journal of Computing and Information Science in Engineering*, 2001, 1(3), 205-217.
- [8] Zhu, F., Visualized CAD modeling and layered manufacturing modeling for components made of a multiphase perfect material, M.Phil. Thesis. The University of Hong Kong, 2004.
- [9] Elishakoff, I., Gentilini, C. and Viola, E., Three-dimensional analysis of an all-round clamped plate made of functionally graded materials, *Acta Mechanica*, 2005, 180(1-4), 21-36.
- [10] Siu, Y.K. and Tan, S.T., Source-based heterogeneous solid modeling, *Computer-Aided Design*, 2002, 34(1), 41-55.
- [11] Biswas, A., Shapiro, V. and Tsukanov, I., Heterogeneous material modeling with distance fields, *Computer-Aided Geometric Design*, 2004, 21(3), 215-242.
- [12] Liu, H., Maekawa, T., Patrikalakis, N.M., Sachs, E.M. and Cho, W., Methods for feature-based design of heterogeneous solids, *Computer-Aided Design*, 2004, 36(12), 1141-1159.
- [13] Samanta, K. and Koc, B., Feature-based design and material blending for freeform heterogeneous object modeling, *Computer-Aided Design*, 2005, 37(3), 287-305.

- [14] Qian, X. and Dutta, D., Design of heterogeneous turbine blade, *Computer-Aided Design*, 2003, 35(3), 319-329.
- [15] Pasko, A., Adzhiev, V., Schmitt, B. and Schlick, C., Constructive hypervolume modeling, *Graphical Models*, 2001, 63(6), 413-442.
- [15] Bibb, R. and Sias, G., Bone structure models using stereolithography: a technical note, *Rapid Prototyping Journal*, 2002, 8(1), 25-29.
- [16] Chen, Z.Z., Li, D.C., Lu, B.H., Tang, Y.P., Sun, M.L. and Wang, Z., Fabrication of artificial bioactive bone using rapid prototyping, *Rapid Prototyping Journal*, 2004, 10(5), 327-333.
- [17] Sun, W., Starly, B., Darling, A. and Gomez, C., Computer-aided tissue engineering: application to biomimetic modeling and design of tissue scaffolds, *Biotechnology and Applied Biochemistry*, 2004, 39(1), 49-58.
- [18] Fang, Z.-B., Starly, B., Shokoufandeh, A., Regli, W. and Sun, W., A computer-aided multi-scale modeling and direct fabrication of bone structure, *Computer-Aided Design and Applications*, 2005, 2(5), 627-634.
- [19] Bhashyam, S., Shin, K.H., Dutta, D., An Integrated CAD system for design of heterogeneous objects, *Rapid Prototyping Journal*, 2000, 6(2):119-135.
- [20] Fessler, J., Nickel, A., Link, G., Prinz, F., Fussell, P., Functional gradient metallic prototypes through shape deposition manufacturing. Solid Freeform Fabrication Proceedings, Austin, TX. 1997. 521-528.
- [21] Li, X.C., Choi, H. and Yang, Y., Micro rapid prototyping system for micro components, *Thin Solid Films*, 2002, 420-421,515-523.
- [22] Wang, F., Chen, K. Feng, X. and Feng, X., Developing a manufacturing technology for the components made of a multiphase perfect material, *International Journal of Advanced Manufacturing Technology*, 2009,40(7-8),837-846
- [23] Sachs, E., Haggerty, J., Cima, M. and Williams, P. Three-dimensional printing techniques. U.S. Patents, 5,204,055. 1993.
- [24] Sachs, E., Wylonis, E., Allen, S., Cima, M. and Guo, H. Production of injection molding tooling with conformal cooling channels using the three dimensional printing process , *Polym Eng Sci*, 2000, 40(5), 1232- 1247.
- [25] Curodeau, A., Sachs, E. and Caldarise, S. Design and fabrication of cast orthopedic implants with freeform surface textures from 3-D printed ceramic shell, *J Biomed Mater Res*, 2000, 53(5), 525-535.

- [26] Koch, J. and Mazumder, J. Rapid prototyping by laser cladding, Proceedings of SPIE, 1993.
- [27] Mazumder, J., Dutta, D., Kikuchi, N. and Ghosh, A., Closed loop direct metal deposition, art to part, *Opt. Lasers Eng.* 2000, 34(4-6), 397-414.
- [28] Shin, K.H, Natu, H., Datta, D. and Mazumder, J. A method for the design and fabrication of heterogeneous objects, *Materials and Design*, 2003, 24(5), 339-353.
- [29] Keicher, D.M., Miller, W.D., Smugeresky, J.E. and Romero, J.A, Laser engineering net shaping (LENSTM): beyond rapid prototyping to direct fabrication, Proceedings of the 1998 TMS Annual Meeting, 1998, 369-377.
- [30] Keicher, D.M. and Miller, W.D, LENS moves beyond RP to direct fabrication, *Metal Powder Report*, 1998, 53(12), 26-28.
- [31] Griffith, M., Harwell, L., Romero, J., Schlienger, E., Atwood, C. and Smugeresky J. Multi-material processing by LENS. Solid Freeform Fabrication Proceedings, 1997, 387-394.
- [32] Fuesting, T., Brown, L., Das, S., Harlan, N., Lee, G., Beaman, J., Bourell, D., Barlow, J. and Sargent, K., Development of direct SLS processing for production of cermet composite turbine sealing components, Solid Freeform Fabrication Symposium Proceedings, 1996, 39-55.
- [33] Jepson, L., Beaman, J. and Bourell, D., SLS processing of functionally gradient materials, Proceedings of Solid Freeform Fabrication Symposium, 1997, 67-80.
- [34] Beaman, J., Bourell, D., Jackson, B., Jepson, L., McAdams, D., Perez, J. and Wood, K., Multi-material selective laser sintering: empirical studies and hardware development, Proceedings of the 2000 NSF Design and Manufacturing Grantees Conference, 2000.
- [35] Lappo, K., Jackson, B., Wood, K., Bourell, D.L. and Beaman, J.J., Discrete multiple material selective laser sintering (M2SLS): experimental study of part processing, Solid Freeform Fabrication Symposium, 2003, 109-119.
- [36] Bi, Z. M. and Zhang, W.J., Flexible fixture design and automation: Review, issues and future direction, *International Journal of Production Research*, 2001, 39(13), 2867-2894.
- [37] Kang, X and Peng, Q., Fixture feasibility: methods and techniques for fixture planning, *Computer-Aided Design and Applications*, 2008, 5(1-4), 424-433.

- [38] Kruth ,J.P., Wang, X., Laoui ,T. and Froyen L., Lasers and materials in selective laser sintering, *Assembly Automation*, 2003, 23(4), 357-371.
- [39] Sachs, E., Wylonis, E., Allen, S., Cima, M. and Guo, H., Production of injection molding tooling with conformal cooling channels using the three dimensional printing process, *Polymer Engineering & Science*, 2000, 40(5), 1232-1247.
- [40] Huang, X., Ye, C., Wu, S., Guo, K. and Mo, J., Sloping wall structure support generation for fused deposition modeling, *The International Journal of Advanced Manufacturing Technology*, 2009, 42(11-12), 1074-1081.
- [41] Ziemian, C. W. and Crown III, P. M., Computer aided decision support for fused deposition modeling, *Rapid Prototyping Journal*, 2001, 7(3), 138-147.
- [42] Strano, G., Hao, L., Everson, R. M. and Evans, K. E., A new approach to the design and optimisation of support structures in additive manufacturing, *The International Journal of Advanced Manufacturing Technology*, 2013, 66(9-12), 1247-1254.
- [43] Giannatsis, J. and Dedoussis , V., Decision support tool for selecting fabrication parameters in stereolithography, *The International Journal of Advanced Manufacturing Technology*, 2007, 33(7-8), 706-718.
- [44] Zhou, C., Chen, Y., Yang, Z. G., and Khoshnevis, B., Development of Multi-Material Mask-Image-Projection-Based Stereolithography for the Fabrication of Digital Materials, Annual Solid Freeform Fabrication Symposium,2011, 65-80.
- [45] <http://digfablab.wikispaces.com/Envisiontec+Perfactory+RP> (accessed March 20<sup>th</sup> 2013).
- [46] Campbell, R.I., Martorelli, M. and Lee, H.S., Surface roughness visualization for rapid prototyping models, *Computer-Aided Design*, 2002, 34(10), 717-725.
- [47] Pandey, P.M., Reddy, N.V. and Dhande, S.G., Improvement of surface finish by staircase machining in fused deposition modeling, *Journal of Materials Processing Technology*,2003, 132 (1-3), 323-331.
- [48] Armillotta, A., Assessment of surface quality on textured FDM prototypes, *Rapid Prototyping Journal*, 2006, 12 (1), 35-41.
- [49] Joneja, A. and Chang, T.C., Setup and fixture planning in automated process planning systems, *IIE Transactions*, 1999, 31(7), 653-665.
- [50] Tseng, Y.J., Fixturing design analysis for successive feature-based machining, *Computers in Industry*, 1999, 38(3), 249-262.

- [51] Gandhi, M.V. and Thompson, B.S., Phase change fixturing for flexible manufacturing systems, *Journal of Manufacturing Systems*, 1985, 4(1), 29-39.
- [52] Gandhi, M.V., Thompson, B.S. and Maas, D.J., Adaptable fixture design: an analytical and experimental study of fluidized-bed fixturing, *Journal of Mechanisms Transmissions and Automation in Design*, 1986, 108(1), 15-21.
- [53] Choi, D.S., Lee, S.H., Shin, B.S., Whang, K.H., Yoon, K.K. and Sarma, S.E., A new rapid prototyping system using universal automated fixturing with feature-based CAD/CAM", *Journal of Materials Processing Technology*, 2001, 113(1), 285-290.
- [54] Shin, B.S, Yang, D.Y., Choi, D.S., Lee, E.S. Je, T.J. and Whang, K.H., A new rapid manufacturing process for multi-face high-speed machining, *The International Journal of Advanced Manufacturing Technology*, 2003, 22(1-2), 68-74.
- [55] <http://www.deskproto.com/support/videos-venus.htm> (accessed March 23<sup>th</sup> 2013).
- [56] <http://www.rolanddga.com/products/milling/mdx540/#overview> (accessed March 23<sup>th</sup> 2013).
- [57] Boonsuk, W. and Frank, M.C, Automated fixture design for a rapid machining process, *Rapid Prototyping Journal*, 2009, 15(2), 111-125.
- [58] Xu, F., Loh, H.T. and Wong, Y.S. Considerations and selection of optimal orientation for different rapid prototyping systems. *Rapid Prototyping Journal* 1999, 5(2), 54-60.
- [59] Byun, H.S. and Lee, K.H., Determination of the optimal build direction for different rapid prototyping processes using multi-criterion decision making, *Robotics and Computer-Integrated Manufacturing*, 2006, 22 (1), 69-80.
- [60] Cheng, W., Fuh, J.Y.H., Nee, A.Y.C, Wong, Y.S., Loh, H.T. and Miyazawa, T., Multi objective optimization of part building orientation in Stereolithography, *Rapid Prototyping Journal*, 1995, 1(4), 12-23.
- [61] Hur, J. and Lee, K., The development of a CAD environment to determine the preferred build-up direction for layered manufacturing, *International Journal of Advanced Manufacturing Technology*, 1998, 14(4), 247–254.
- [62] Byun, H.S. and Lee, K.H., Determination of the optimal build direction in layered manufacturing using a genetic algorithm, *International Journal of Production Research*, 2005, 43(13), 2709-2724.
- [63] Richard, D.T. and Crawford, R.H., Optimizing part quality with orientation, Solid Freeform Fabrication Symposium, 1995.

- [64] Padhye, N. and Deb, K., Multi-objective optimization and multi-criteria decision making in SLS using evolutionary approaches, *Rapid Prototyping Journal*, 2011,17(6), 458-478.
- [65] Alexander, P., Allen, S. and Dutta, D., Part orientation and build cost determination in layered manufacturing, *Computer-Aided Design*, 1998, 30(5), 343-356.
- [66] Massod, S. H., Rattanawong, W. and Iovenitti, P., Part build orientations based on volumetric error in fused deposition modeling, *International Journal of Advanced Manufacturing Technology*, 2000, 16(3), 162-168.
- [67] Rattanawong, W., Masood, S. H. and Iovenitti, P., A volumetric approach to part-build orientation in rapid prototyping, *Journal of Material Processing Technology*, 2001, 119(1-3), 348-353.
- [68] Lin, F., Sun, W. and Yan, Y., Optimization with minimum process error for layered manufacturing fabrication. *Rapid Prototyping Journal*, 2001, 7(2), 73-81.
- [69] Hebbal, S.S. and Mehta, N.K., Setup planning for machining the features of prismatic parts. *International Journal of Production Research*, 2008, 46(12), 3241-3257.
- [70] Ferreira, P. M. and Liu, C. R, Generation of workpiece orientations for machining using a rule-based system, *Robotics and Computer-Integrated Manufacturing*, 1988, 4(3-4),545-555.
- [71] Ong, S. K., Ding, J., and Nee, A. Y. C., Hybrid GA and SA dynamic setup planning optimization, *Int. J. Prod. Res.*, 2002, 40(18), 4697-4719.
- [72] Ong, S.K. and Chew, L.C., Evaluating the manufacturability of machined parts and their setup plans. *Int. J. Prod. Res.*, 2000, 38(11), 2397-2415.
- [73] Boerma, J.R. and Kals, H.J.J. FIXES, a system for automatic selection of set-ups and design of fixtures, *CIRP Annals - Manufacturing Technology*,1988, 37(1), 443-446.
- [74] Ong, S. K. and Nee, A.Y.C. Application of fuzzy set theory to set-up planning. *CIRP Annals-Manufacturing Technology*, 1994, 43(1), 137-144.
- [75] Ong, S. K. and Nee, A. Y. C. Fuzzy-set-based approach for concurrent constraint set-up planning. *Journal of Intelligent Manufacturing*, 1996, 7(2), 107-120.
- [76] Zhang, H. C. and Huang, S. H. A fuzzy approach to process plan selection. *International Journal of Production Research*, 1994, 32(6), 1265-1279.
- [77] Zhao, Z., Process planning with multi-level fuzzy decision-making. *Computer Integrated Mfg Systems*, 1995, 8(4), 245-254.

- [78] Gan, J. G., Woo, T. C., and Tang, K., Spherical maps: their construction, properties, and approximation, *J. Mech. Des.*, 1994, 116(2), 357-363.
- [79] Suh, S. H., and Kang, J. K., Process planning for multi-axis NC machining of free surfaces, *Int. J. Prod. Res.*, 1995, 33(10), 2723-2738.
- [80] Tang, K., Woo, T., and Gan, J., Maximum Intersection of spherical polygons and workpiece orientation for 4-and 5-Axis machining, *ASME J.Mech. Des.*, 1992, 114(3), 477-485.
- [81] Chen, L. L., Chou, S. Y., and Woo, T. C., Separating and intersecting spherical polygons: computing machinability on three-, four-, and five-axis numerically controlled machines, *ACM Trans. Graph.*, 1993, 12(4), 305-326.
- [82] Radzevich, S.P. and Goodman, E.D., Computation of optimal workpiece orientation for multi-axis NC machining of sculptured part surfaces, *ASME Journal of Mechanical Design*, 2002, 124(2), 201-212.
- [83] Gupta ,P., Janardan, R., Majhi, J. and Woo, T., Efficient geometric algorithms for workpiece orientation in 4- and 5-axis NC-machining, Proc. 4th Workshop Algorithms Data Struct, 1995, 955, 171-182.
- [84] Li, Y. and Frank, M.C., Computing Axes of Rotation for Setup Planning Using Visibility of Polyhedral CAD Models, *Journal of Manufacturing Science and Engineering, Transactions of the ASME*, 2012,134(4), 041005(1-10).
- [85] Mazumder, J., Koch, J., Nagarathnam, K., and Choi, J., Rapid manufacturing by laser aided direct deposition of metals, *Advances in Powder Metallurgy and Particulate Materials 4*, 1996, 15-107.
- [86] Mazumder, J., Choi, J., Nagarathnam, K., Koch, J., and Hetzner, D., The direct metal deposition of H13 tool steel for 3-D components, *JOM*, 1997,49(5), 55-60.
- [87] Fessler, J., Nickel, A., Link, G., Prinz, F., and Fussell, P., Functional gradient metallic prototypes through shape deposition manufacturing, 8<sup>th</sup> Annual Solid Freeform Fabrication Symposium, 1997, 521-528.
- [88] Merz, R., Prinz, F. B., Ramaswami, K., Terk, M., and Weiss, L., Shape deposition manufacturing, 4th Annual Solid Freeform Fabrication Symposium, 1994, 1-8.
- [89] Griffith, M., Harwell, L., Romero, J., Schlienger, E., Atwood, C., and Smugeresky, J., Multi-material processing by LENS, 8<sup>th</sup> Annual Solid Freeform Fabrication Symposium, 1997, 387-394.

- [90] Lewis, G., and Nemea, R., Properties of Near-Net Shape Metallic Components Made by the Directed Light Fabrication Process, 8<sup>th</sup> Annual Solid Freeform Fabrication Symposium, 1997, 513-520.
- [91] Sachs, E., Haggerty, J., Cima, M., and Williams, P., Three-dimensional printing techniques, U.S. Patent No. 5,204,055, 1993.
- [92] Shin, K.H. and Dutta, D., Process-planning for layered manufacturing of heterogeneous objects using direct metal deposition, *Journal of Computing and Information Science in Engineering*, 2002, 2(4), 330-344.
- [93] Xu, A. and Shaw, L., SFF-oriented modeling and process planning of functionally graded materials using a novel equal distance offset approach, Proceedings of Solid Freeform Symposium, 2004, 544-552.
- [94] Xu, A. and Shaw, L.L., Equal distance offset approach to representing and process planning for solid freeform fabrication of functionally graded materials, 2005, *Computer-Aided Design*, 37(12), 1308-1318.
- [95] Deuser, B., Tang, L., Geldmeier, J., Landers, R.G., and Leu, M.C., Process planning and control for functionally graded material fabrication using freeze-form extrusion fabrication, Proceedings of Solid Freeform Symposium, 2011, 415-426.
- [96] Maruo, S., Ikuta, K. and Ninagawa, T., Multi-polymer microstereolithography for hybrid opto-MEMS, Proceedings of the 14th IEEE International Conference on Micro Electro Mechanical Systems, 2001, 151-154.
- [97] Kim, H., Choi, J., and Wicker, R., Scheduling and process planning and for multiple material stereolithography, *Rapid Prototyping Journal*, 2010, 16(4), 232-240.
- [98] Kim, H., Choi, J., MacDonald, E., and Wicker, R., Slice overlap detection algorithm for the process planning of multiple material stereolithography apparatus, *The International Journal of Advanced Manufacturing Technology*, 2010, 46(9), 1161-1170.
- [99] Zhou, C., Chen, Y., Yang, Z. G., and Khoshnevis, B., Development of multi-material mask-image-projection-based stereolithography for the fabrication of digital materials, Annual Solid Freeform Fabrication Symposium, 2011, 65-80.
- [100] Choi, S.H., and Cheung, H.H., A multi-material virtual prototyping system for product development and biomedical engineering, *Computer-Aided Design and Applications*, 2005, 2(1-4), 329-338.
- [101] Choi, S.H., Cheung, H.H., A versatile virtual prototyping system for rapid product development, *Computers in Industry*, 2008, 59(5), 477-488.

[102] Chen, K.Z., Feng, X.Y., Wang, F. and Feng, X.A., A virtual manufacturing system for components made of a multiphase perfect material, *Computer-Aided Design*, 2007, 39(2),112-124.

## CHAPTER 3. A METHOD TO REPRESENT HETEROGENEOUS MATERIALS FOR RAPID PROTOTYPING – THE MATRYOSHKA APPROACH

**Shuangyan Lei, Matthew C. Frank, PhD**

Department of Industrial and Manufacturing Systems Engineering,  
Iowa State University, Ames, IA, USA

**Donald D. Anderson, PhD and Thomas D. Brown, PhD**

Department of Orthopaedics and Rehabilitation  
The University of Iowa, Iowa City, IA, USA

A paper in the Rapid Prototyping Journal, 2014, 20(5), *accepted, to appear*

### **Abstract**

**Purpose** - The purpose of this paper is to present a new method for representing heterogeneous materials using nested STL shells, based in particular on the density distributions of human bones.

**Design/methodology/approach** - Nested STL shells, called *Matryoshka* models, are described based upon their namesake Russian nesting dolls. In this approach polygonal models, such as STL shells, are “stacked” inside one another to represent different material regions. The *Matryoshka* model addresses the challenge of representing different densities and different types of bone when reverse engineering from medical images. The *Matryoshka* model is generated via an iterative process of thresholding the Hounsfield Unit (HU) data from a computed tomography (CT) scan, thereby delineating regions of progressively increasing bone density. These nested shells can represent regions starting with the medullary (bone marrow) canal, up through and including the outer surface of the bone.

**Findings** - The *Matryoshka* approach introduced can be used to generate accurate models of heterogeneous materials in an automated fashion, avoiding the challenge of hand-creating an assembly model for input to multi-material additive or subtractive manufacturing.

**Originality/Value** - This paper presents a new method for describing heterogeneous materials: in this case, the density distribution in a human bone. The authors show how the *Matryoshka* model can be used to plan harvesting locations for creating custom rapid allograft bone implants from donor bone. An implementation of a proposed harvesting method is demonstrated, followed by a case study using Subtractive Rapid Prototyping to harvest a bone implant from a human tibia surrogate.

**Keywords** - Rapid prototyping, Rapid manufacturing, Heterogeneous object modeling, Bone implant

**Paper type** - Research paper

### 3.1 Background

Among the extraordinary capabilities of current Additive Manufacturing (AM) is the recent ability to create parts with varying material properties. Some example AM techniques include Three Dimensional Printing (3DP), Laser Engineered Net Shaping (LENS), and Polyjet Technologies, which can make parts with multiple materials, or at least designate multiple components in color (3DP). In particular, the multi-material 3D printing system Connex500™ developed by Objet Ltd. has the capability of printing

parts made of up to fourteen different materials in a single print. Multi-material or *heterogeneous* materials, in general, involve objects with spatially different material compositions or structures [1,2]. Recently, heterogeneous components have attracted research interest, and extensive work has been undertaken in the area of heterogeneous object modeling in CAD.

Simultaneously, there has also been considerable research in the biomedical and Rapid Prototyping (RP) communities to address the challenge of creating custom bone implants. Biomedical implant manufacturing using AM has made significant progress in fabricating patient-specific implants. These techniques include Selective Laser Melting (SLM), Stereolithography (SLA), Electron Beam Melting (EBM), Direct Metal Laser Sintering (DMLS), 3DP, LENS, etc. SLM has been shown to be a useful process to manufacture 3D porous metallic structures using a variety of material options, including stainless steel, titanium, and chromium-cobalt [3]. EBM technology has been relatively widely used to fabricate custom-designed implants for knees, hips, elbows, shoulders, fingers, and bone plates in titanium alloy (Ti6Al4V) [4,5]. LENS has also been developed to make load-bearing metal porous implants with complex anatomical shapes from materials like Ti, Ti6Al4V, Ni-Ti and CoCrMo alloys. The surface porosities and load-bearing properties of such manufactured implants depend on parameters like laser power, power feed rate, and scan speed [6-8]. SLA can be used to create tissue geometry of arbitrary 3D shapes directly from CAD data, and low-density cellular materials with gaseous voids have been manufactured by SLA technologies [9]. This cellular structure material facilitates bone ingrowth for biological fixation, such as the

case with acetabular implants designed with preferential porosity gradients for use in hip replacement [10].

Existing CAD models investigating this topic fall into two categories, which are *evaluated* models and *unevaluated* models, depending on the representational exactness and compactness [11]. Evaluated models are inexact, and represent heterogeneous materials distributions through intensity-space decompositions. Typical examples are the voxel models [12,13] and volume mesh based models [14]. Unevaluated models utilize exact geometric data representation and rigorous functions to represent the material distributions. Examples include explicit functional representations [15-17], control feature-based models [18-21], control point-based models [22], and implicit function-based models [23].

A variety of heterogeneous object modeling methods have been presented in the literature; however, challenges remain with representation of the complex models that RP systems can manufacture. This is true not only for multi-materials, but for other complex geometries in general. For example, additive RP machines can create complex scaffolds, but new methods are still under development for easy and computationally efficient representation of models such as bone scaffolds, biomimetic objects, etc.

One particularly challenging heterogeneous materials is bone. Clinically, at present, there is very strong preference for usage of native bone to reconstruct defects commonly resulting from severe trauma, from excision of bone tumors, and from biologically mediated loss of bone around failed or failing joint replacements. The

patient's own bone (an autograft) is most preferred for such purpose, but options for sites from which to harvest autograft obviously are very limited. Bone from a deceased donor (allografts) is by far the most commonly used alternative. Surgeons often are faced with the problem of shaping part of an allograft donor bone to fit an irregularly shaped defect in a living patient's bone, configuring the allograft so as to approximately match the patients' original density distribution.

Native human bone's density distribution from inside to outside spans a significant range. To illustrate, Figure 1 shows a cross sectional view of a femur bone, showing the spongy, low density trabecular bone in the middle, versus the high-density cortical bone on the outside. There have been numerous

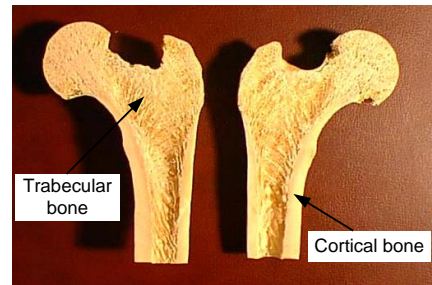


Figure 1. A cross-sectional view of a femur bone.

research efforts to model the density of bone. For example, Yao and Taylor used a Bernstein polynomial in barycentric coordinates to model density variations [24]. Bibb and Sias used SLA techniques to build cancellous bone structure models, and investigated the problems associated with the CAD models saved in STK and SLC file formats, respectively [25]. Chen et al. [26] put forward a technique to fabricate the mold of an artificial bone, composed of a nontoxic soluble material, by using two CAD models: an external contour CAD model, and an internal microtubule structure CAD model. The external contour model is obtained by reconstructing the 3D geometry from bone CT scan data and saved to STL format. The internal microtubule structure model was built up through micrographs and histological analysis. Fang et al. [27] proposed a

multi-scale voxel modeling approach to model the bone structure at macroscopic and microscopic levels, and developed a Direct Fabrication (DF) system to fabricate a tissue scaffold constructed with a random heterogeneous microstructure and designed shape. Sun et al. [28] presented a method to develop a femur model by using quantitative CT numbers (QCTN) to characterize the bone mechanical properties. It used different QCTN to characterize the density of the tissue in different layers and considered both cancellous and cortical bone smeared together as one structure in each layer.

Currently, there is no effective modeling approach to characterize the heterogeneity of bone structure, let alone any method that would enable automated process planning in a rapid prototyping system. This paper focuses on the challenge of representing multi material bone properties from CT scan data, a widely used medical imaging modality that represents x-ray attenuation properties (which scale with density) as grayscale image intensity distributions (Figure 2).

Bone implants or bone grafts are widely used in the treatment of severe fractures or in tumor removal to replace a damaged or missing piece of bone. In order for the human body to accept the bone implant material and heal properly, it is essential that the bone implant be both mechanically and biologically compatible. Such

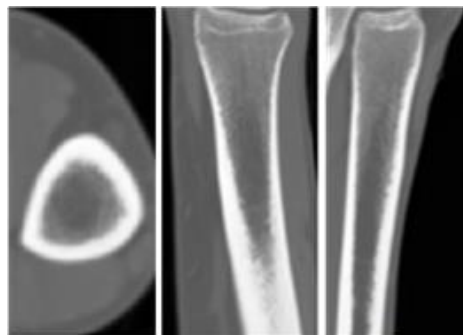


Figure 2. CT slices along different axes [29].

implants can be made from various artificial bone materials, or from natural bone, in the form of allograft obtained from a donor, or an autograft taken from another bone of the

patient. In any case, there arises the challenge of having correctly shaped implants created from an appropriate material, in a timely manner. Currently, during surgery, this challenge is met through the hand-shaping by the surgeon.

Even in the current era of sophisticated bone grafting procedures, advanced synthetic biomaterials and bioactive/tissue engineered implants, refined capabilities for restoring soft tissue coverage, and highly evolved distraction osteogenesis techniques [30], treating segmental bone defects presents a major challenge. To date, most attention in this area has focused on mid-shaft long bone defects, where the principal reconstructive objective is to achieve bone healing with nominal preservation of limb length and alignment. While shape matching between the graft and the recipient site is always desirable in principle, many mid-shaft fractures are relatively forgiving in that regard. Various other bone defects, by contrast, place a much higher premium on close geometrical matching of the graft. For example, bone defects associated with severe articular or peri-articular fractures (i.e., fractures near a joint such as the knee or hip) requires a substantially higher degree of reconstruction accuracy than is the case for the mid-shaft defects, owing to the need for stable, congruous articulation of the joint surface. Bone healing of an articular fracture in other than closely anatomic position predisposes the joint to secondary arthritis, a major contributing factor to poor outcomes, whose morbidity frequently approaches that of amputation [31].

At the local macroscopic level, all fractures possess individual geometric signatures. Current synthetic implant or grafting strategies for achieving healing of segmental defects offer only limited opportunity to address individualized defect geometry, since

they have evolved mainly for situations (mid-shaft defects) where close reconstruction of local geometry is not particularly critical. Using conventional methods, there has to be primary reliance on fixation hardware to hold the respective bone surfaces in the desired nominal apposition, with the implant or graft making at best local spot contact with the recipient bone, and with appreciable gaps existing across much if not most of the intended-union interfaces. Even with the most advanced contemporary fixation in the hands of highly trained orthopaedic traumatologists, comminuted peri-articular fractures (especially in the presence of segmental defects) pose a severe biomechanical challenge, which often is not well resisted by usage of conventional bone grafts (Figure 3) [32]. Virtually all contemporary synthetic implant materials, all tissue engineered defect-filling constructs, and especially all variants of bone grafts would have better prospects for achieving optimal outcome if they began from a condition of closely fitting the local geometry of the recipient bone surface(s).

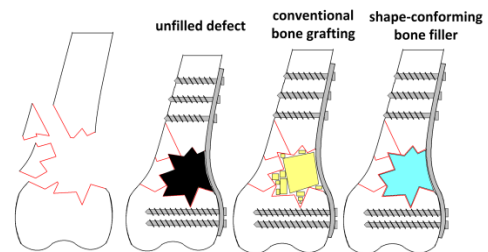


Figure 3. Schematic of a typical bone implant

Although additive RP technologies provide the ability to create complex shapes in some biocompatible materials; other approved and desired materials are not usable, in particular, natural bone. Allograft bone holds strong preferential attraction over artificial biocompatible materials in many situations clinically [33, 34]. However, two challenges need to be overcome in order to permit automated shape machining of allograft bone. The first challenge is that, unlike engineered materials for which the source machining

stock is in the convenient form of geometrically regular shapes such as cylinders or rectangular blocks, for allografts the source material is necessarily restricted to irregularly-shaped donor bones. The second prelude challenge is that, unlike for homogeneous artificial source materials for which the implant could be machined from anywhere arbitrarily within the original stock, for the case of donor bones the site and orientation of implant harvest need to respect the realities of heterogeneous internal bony architecture. From the clinical perspective, harvesting and creating implants from allograft bone still presents significant challenges.

To summarize, the previous research in this area leaves two related and somewhat dependent challenges, which provide the scope for this current work. One, the problem of representing heterogeneous materials is generally not addressed sufficiently today. Two, the more specific challenge of creating amorphous shaped heterogeneous components like bone implants is either unavailable or done completely by hand. To address these challenges, this paper first proposes an approach for compactly representing heterogeneous bony anatomy, and then a harvesting method that utilizes that approach to automate subtractive rapid prototyping of allograft bone implants working from CT scan data.

### **3.2 The *Matryoshka* Shell Model**

This work proposes a novel way to create heterogeneous models of natural bone using a series of stacked shells. As such, the namesake "*Matryoshka*" is borrowed from the novelty Russian "nesting dolls." This stacked shell paradigm is used to describe the

bone density distribution using discrete regions generated from normative CT image data. As a simple example, Figure 4(a) shows a set of *Matryoshka* nested dolls. The salient characteristic of Russian nesting dolls is that the size of each nested doll decreases in order to place one inside the other, as shown in Figure 4(b). Although models generated from bones will not always follow the monotonically decreasing regions of these dolls, the general concept of nested shells is appropriate for most long bones used to provide allografts (e.g., femurs, tibias, etc.).

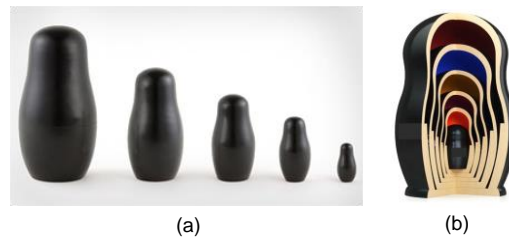


Figure 4. *Matryoshka* shell model. (a) Set of *Matryoshka* dolls, in order of size [35] and (b) Cut-away view of nested *Matryoshka* dolls [36].

The motivation behind the *Matryoshka* models used in this work is to provide a search space from within a proper harvesting site from which a bone implant can be found. This concept was shown in previous work focused on developing methods to create custom bone implants from donor bone, with implant geometries derived from CT scanning of bones [37]. The process of creating an implant begins with a CT scan of the fracture site, tumor resection site, etc., and then a computational reconstruction of the missing and/or unusable portion of bone. The resulting CAD geometry can be used in Subtractive Rapid Prototyping (SRP) to machine the implant from stock. Figure 5 shows a series of trial prototype implants created using SRP on a variety of materials

representing clinically relevant properties. The niche application of SRP lies in a relatively few materials, namely FDA-approved biomaterials like Trabecular Metal, or, of particular significance, natural allograft bone from a tissue bank. Allograft bone specifically motivates the need for a heterogeneous material modeling method; hence, it is the focus of this current work.

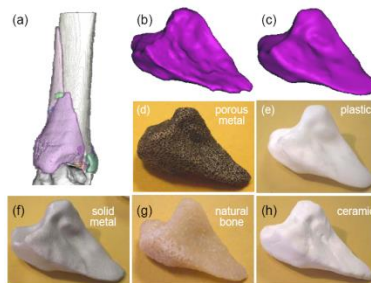


Figure 5. Sample implant materials from a variety of clinically relevant materials. (a) Segmented CT image showing various fragments; (b) Individual computational fragment image as extracted, and (c) as computationally smoothed; (d-h) Corresponding 3D fragment geometries created using SRP from Trabecular Metal®, plastic, solid metal, bovine bone, and porous ceramic.

This work proposes using a simple method to evaluate and directly model the density of a given bone sample, namely through CT scanning. The Hounsfield Unit (HU), which indexes X-ray attenuation, indicates the varying levels of bone density; high HU corresponds to high density, and vice versa. HUs are also associated with grayscale of the CT slice image, which carries intensity information. By setting threshold HU values, pixel values below given threshold values can be identified as pixels-of-interest, while HU values above the threshold values can be identified as background pixels. Figure 6

shows an example of distinguishing pixels of interest from a CT slice image, using the HU threshold method. In this example, one can create different contours for each image. Hence, the CT slice image can be divided into five different regions bounded by different contours. When each increasing contour shell is created, it is assumed that the pixels within that region have a common singular HU around the threshold value. In this manner, the continuous bone density function exhibited on the CT slice can be discretized into a step function. Straightforward extension of an iterative thresholding operation on a series of CT slices allows one to stack them together, and a 3D nested shell model can be created: the Matyroska model.

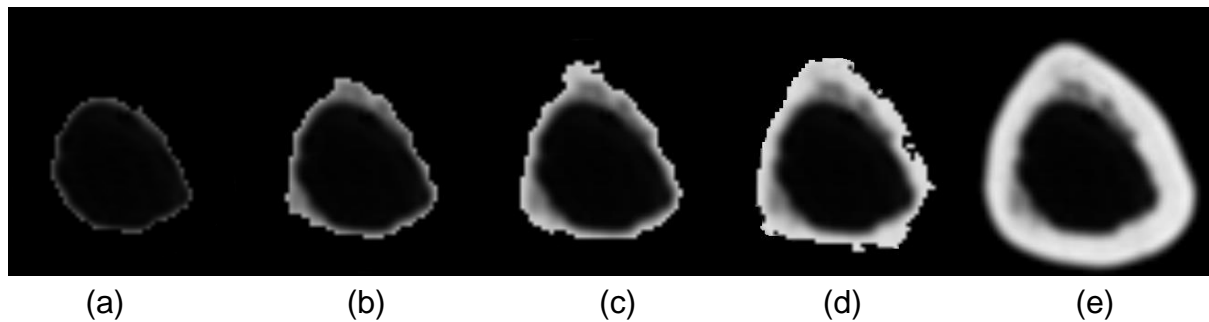


Figure 6. Distinguishing the pixels of interest from the CT slice image by the HU threshold method. (a)  $HU \leq 1203$ ; (b)  $HU \leq 2277$ ; (c)  $HU \leq 2768$ ; (d)  $HU \leq 2982$ ; (e)  $HU \leq 3140$ .

An example of a *Matryoshka* model for a human tibia is shown in Figure 7. This model was constructed of five shells: an innermost medullary cavity shell (Shell 1), a low-density cancellous bone shell (Shell 2), a high-density cancellous bone shell (Shell 3), a cortical bone shell (Shell 4), and a bone outer surface (Shell 5). In this way, the entire 3D volume of the bone is classified as being within one of four bone regions, bounded

by five shells. Although the general method applies for any surface model or polygonal file format, the present work uses the .PLY file format. The PLY format was chosen for its ability to convey color information, which is not possible with the STL file format. Of course, the new Additive Manufacturing File Format (AMF) affords color, material, and much more information, and could be used instead of PLY formatting. However, even if an AMF file format were used, one would still need appropriate definitions of the material properties throughout the bone. As an alternative to doing this manually, a method is proposed here for creating the shells and automatically defining the material properties *a-priori*.

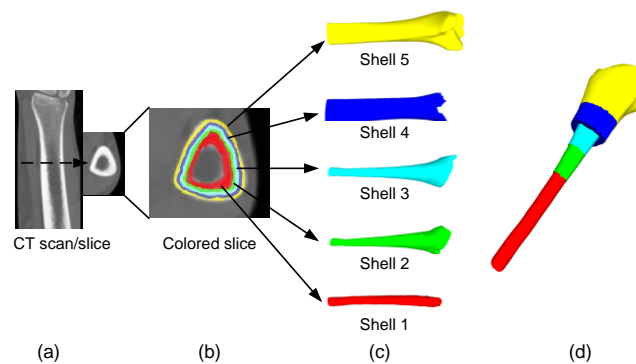


Figure 7. *Matryoshka* model of the human tibia. (a) CT Scan and slice; (b) View of colored cross-sectional geometry; (c) Five shells generated from the medullary canal to outer bony surface; (d) Cut-away view of an assembled final model.

The proposed method can automatically generate a model through an iterative process from a CT scan, rather than requiring manual construction by the user. In an additive manufacturing system, this might include assigning differing process parameters for

each region, or simply choosing different material formulations. By contrast, the niche area of Subtractive Rapid Prototyping is particularly appropriate, where automatically planning for custom natural bone implants is the overarching challenge. Although previous research has applied rapid machining (CNC-RP) to fully automated process planning for industrial components [38-43] the challenge of rapid machining of natural bone begins with choosing a proper “harvesting” location from which to extract the bony geometry of the implant from within the donor bone. In other words, one is faced with the challenge of finding a suitable location from which to machine an arbitrary free-form shaped object from within another arbitrary free-form shaped stock material object, where each has a unique material density distribution. Figure 8 illustrates an example of this type of implant harvest. Figure 8(a) shows the CT-derived CAD model of the desired implant (with added holes for fixation screws), while Figure 8(b) shows a surrogate bone human tibia. Lastly, Figure 8(c) shows the “harvest” location, where it was deemed best to machine the implant from within the donor bone, based on geometry and density distribution.

Identifying desired implant geometry is facilitated by unique “3D puzzle solving” algorithms and software, which can create accurate 3D CAD model reconstructions of the missing bone directly from CT scan data [44]. This software was originally developed to reassemble a fracture site (i.e., locating and aligning all the puzzle pieces in their proper anatomic position). However, it became apparent that Boolean operations on the “puzzle” solution, compared to a mirrored image of the intact “other” limb (right or left), could reveal the correct geometry of any missing pieces, as well.

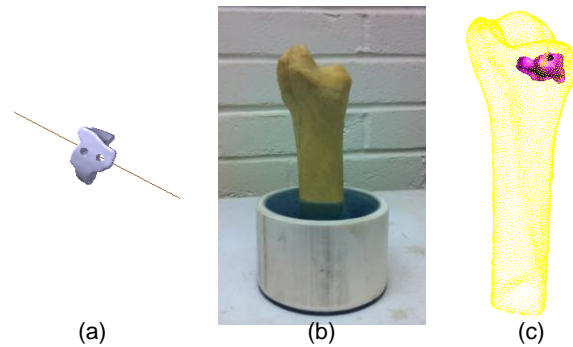


Figure 8. Illustration of harvesting an implant from a desired location within the donor bone. (a) A CAD model of the implant; (b) A surrogate potted tibia bone; (c) The selected harvest location within the donor bone.

The following sections provide an approach to search and evaluate potential implant harvest sites from within a donor bone using a *Matryoshka* shell model. The goal is to automatically define the “goodness” of a location using quantifiable metrics. Currently, an overall bone *Density* score and/or a *Similarity* score are used to provide best locations to achieve highest density and best-matching density distributions, respectively.

### 3.2.1 Using a Matryoshka Model for Bone Implant Harvesting

As a practical matter, human *long bones* (femur, tibia, humerus, etc.) are most attractive as donor bones. Long bones generally have a hard outer surface of compact bone, a spongy inner region comprised of cancellous bone, and bone marrow. If one considers the shape similarity between a long bone and a cylinder, a long bone generally exhibits increasing density as one moves away from the axis radially, or, away from the

medullary canal in the center of the bone. This gives a basis for defining the “center line” of the bone.

It is assumed that both patient bone and donor bone have already been aligned approximately anatomically such that the *anterior*, *posterior*, *proximal*, *distal*, etc. directions correspond to standard views. This assumption is based on experience with medical imaging, whereby radiologists set orientations and describe views in standardized “coordinate systems”, not unlike the way CAD modelers use the terms “front,” “right,” and “side” views in orthogonal projections.

Before initiating a search for the harvesting location within the donor bone, an important first step is to align the “center lines” or axes of the patient bone and donor bone. Thus, the distributions of density in the implant and the donor bone would generally align radially along the same axis. As such, when one traverses a set of cylindrical coordinates in the donor or patient bone space, the gradient directions would generally align (i.e. moving away radially will increase density in both, and vice versa).

The procedure of identifying the “center line” of the donor bone involves straightforward slicing of the shaft of the donor bone and patient bone models. Next, using a least squares method, we fit the centroids of the chains on all of the slices with a linear function (straight line). The straight line is approximated as the “center line” of the donor and patient bones. Figure 10 shows the results of fitting the bone centroids with straight lines.

Next, both bones are aligned to a common Z-axis orientation (Figure 9). At this point, both donor and patient bones are in the same orientation (Figure 9(a)), and although they do not lie on the same axis, they need a common final alignment. Achieving this is simply a matter of uniaxial translation so as to align the ends of the patient and donor bones (Figure 9(b)). Next, the implant geometry is translated into the donor bone space in order to start evaluating possible harvest positions (Figure 9(c)).

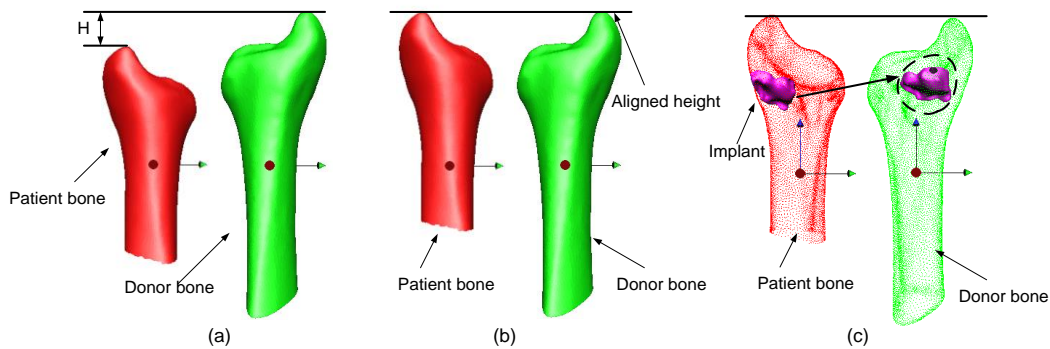


Figure 9. An example of aligning the ends of the bones. (a) Before alignment; (b) After alignment; (c) Implant geometry from patient bone transferred to donor bone.

Searching for the best harvest location involves rotating the implant around the center line of the donor bone, and translating the implant along the center line axis direction and radially toward and away from the center line. Note that the implant is not initially located at the “same” rotation about the centerline axis from where it originated in the patient. The following sections describe an exhaustive search process, demonstrating why this is unnecessary.

### 3.2.2 Creating a Discretized Slice Model

Before the iterative search begins, the space available for potential implant harvesting is discretized through a process enabled by the *Matryoshka* model. A key characteristic of the *Matryoshka* strategy is that the 3D space is reduced to simpler, yet still highly detailed slice information (i.e. the color slice image in Figure 10(a)). The color slice can be considered as a “boundary”; the region within each color boundary is assigned a specific value, representing its density. In this manner, all elements contained between two adjacent shells are set to the same value, other than the first shell, which only contains the medullary canal and is not a feasible region for bone harvesting. As shown in Figure 10(b), values  $a$ ,  $b$ ,  $c$ , and  $d$  represent the bone densities from different regions in the slice model, whereby the continuously varying bone density is discretized into four different regions on the slice that are available as potential harvesting locations. Next, a spider cell structure is used to discretize each slice into a grid of sectors about the  $Z$ -axis, with an interval angle  $\alpha$ , and with each sector further divided by grid elements with interval  $h$ , as shown in Figure 10(c). Each grid element is assigned a specific value indicating the density of the region encompassed by the corresponding grid element. In general, smaller  $\alpha$  and  $h$  will result in a more accurate and finer discretization structure, but at the expense of increased computation time (the grid spacing for both  $\alpha$  and  $h$  are shown excessively coarse in Figure 13(c) for clarity; in practice, they are 1-5° and 1-3 mm, respectively).



Since all grid elements that fall within the surface boundaries of the bone will be assigned to one of the specific density regions, those grid elements temporarily indexed in the array with a value of 0 must be modified to represent the density correctly. For example, after filling in the 0 elements of the array, the updated row of the array is shown in Figure 11(b).

### 3.2.3 Density Score and Similarity Score Calculation

The goal is to assign a quantitative score of “goodness” for a candidate location for bone harvesting. This will involve the density of the implant, regardless of whether the preference is simply for high overall density, or for a highly similar distribution of densities between donor and patient. So, after discretizing the slice model into the grid structure and assigning a density value in each element, the area of each element is determined based on

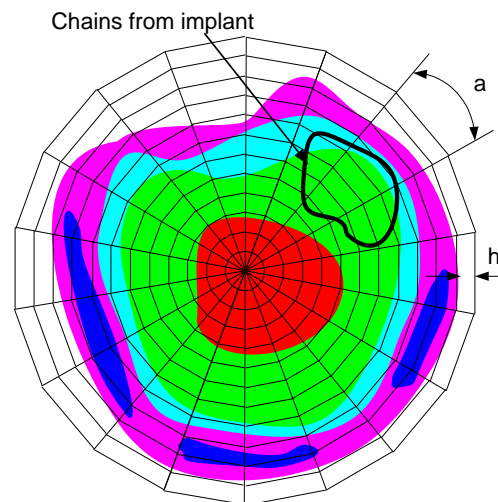


Figure 12. Color mapping in grid structure

parameters  $\alpha$  and  $h$ . Only those elements which are inside of the implant slice chains or which contain implant slice chains are used to calculate the implant density score, as shown in Figure 12.

To calculate the overall effectiveness score for the entire provisional implant position, density metrics are calculated for each chain of each slice for the entire implant, as follows.

Let  $N$  be the total number of slices for the implant, for  $i$  slices from 0 to  $N-1$ . Let  $j$ , ranging from 0 to 3, represent the four bone density regions. Then, let  $S_{ij}$  indicate the area of the different density regions  $j$  on slice  $i$ . Recall that the density regions 0, 1, 2, 3 represent the range from low-density cancellous bone region to the highest density cortical bone region. Then, the area matrix  $S$  is normalized by:

$$S_{ij} = \frac{S_{ij}}{\sum_{i=0}^{N-1} \sum_{j=0}^3 S_{ij}} \quad (1)$$

$i=0, 1, \dots (N-1)$  (slice),  $j = 0, 1, \dots, 3$  (region)

Finally, the density score is calculated by:

$$Density\ score = \sum_{i=0}^{N-1} \sum_{j=0}^3 (S \times A^T) \quad (2)$$

$$A = [a, b, c, d] \quad (3)$$

Using the same procedure, the normalized area matrices  $S$  and  $S'$  are calculated for the donor bone and patient bone, respectively. The similarity score is then calculated by:

$$Similarity\ score = \sum_{i=0}^{N-1} \sum_{j=0}^3 abs(S_{ij} - S'_{ij}) \quad (4)$$

These two scores, *Density* and *Similarity*, can then be used independently or together, to calculate the effectiveness of a provisional harvest site. Whereas *Density* is an

aggregate score for the entire implant, *Similarity* is evaluated slice by slice. Hence, although one could achieve a high overall *Density* score by having some portion of the implant gain density at the expense of another portion losing density, the *Similarity* score will be affected more locally.

Conceptually, the simplest approach is to conduct an exhaustive search of the entire donor bone space to determine the optimal location for the harvested implant. This exhaustive search involves rotating the implant about the Z-axis and translating the implant up and down in the Z-axis direction, all while moving the implant closer to or farther from the Z-axis radially. In other words, the implant is moved at the granularity of the spider grid structure throughout the entire donor bone space. For each iteration, the *Density* and *Similarity* are calculated, and then both values are normalized. In our current implementation, a final attractiveness score is calculated based on a weighted function of the aggregate “goodness” of each feasible solution.

$$\text{Max } \{\alpha \times \text{Normalized}(\text{Density score}) + \beta \times \text{Normalized}(\text{Similarity score})\} \quad (5)$$

Here  $\alpha$  and  $\beta$  are coefficient weights on the importance of *Density* and *Similarity*; these are values which can be assigned by the surgeon, radiologist, tissue bank technician, etc.

### 3.3 Implementation Example

#### 3.3.1 Matryoska Model Generation and Harvesting Search

The algorithms developed in this work have been implemented in C++ and are graphically displayed using *OpenGL*. To illustrate the implementation of these analyses, two sets of human tibia bone CT scan slices are used. These slices were first imported into ITKsnap (open source software) and saved as a voxel array DICOM file. Next, the DICOM data were loaded into Matlab, and the five Matyroshka shells were generated using an increasing Hounsfield Unit cutoff. The created shells were then saved into a PLY file in MATLAB, and imported to RapidForm software for post-processing. Post-processing included correcting the geometric errors in the PLY file (holes, spikes, etc.). The post-processed shells created were the marrow canal (Shell 1), one lower-density cancellous bone (Shell 2), one higher-density cancellous bone (Shell 3), the cortical bone shell (Shell 4) and the outer tibia surface (Shell 5), as shown in Figure 13, listed with the respective HU used to generate them.

One set of the CT scan images had 566 slices, each of 228×264 voxels and within spacing of 0.3 mm. The other set of data had 298 slices of 205×298 voxels, within spacing of 0.5 mm. From each set of CT scan images, a polyhedral PLY file was generated. These PLY files were subsequently used for harvesting analysis. Both patient bone and donor bone models were sliced with 2.0 mm spacing. To create the “spider,” discretization parameters  $\alpha$  and  $h$  were chosen to be 3° and 1.35 mm,

respectively. The overall *Density* score of the implant from within the original patient bone was found to be 435.

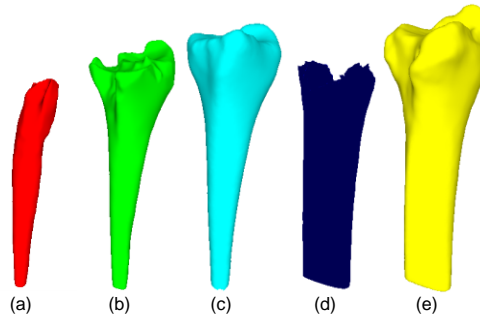
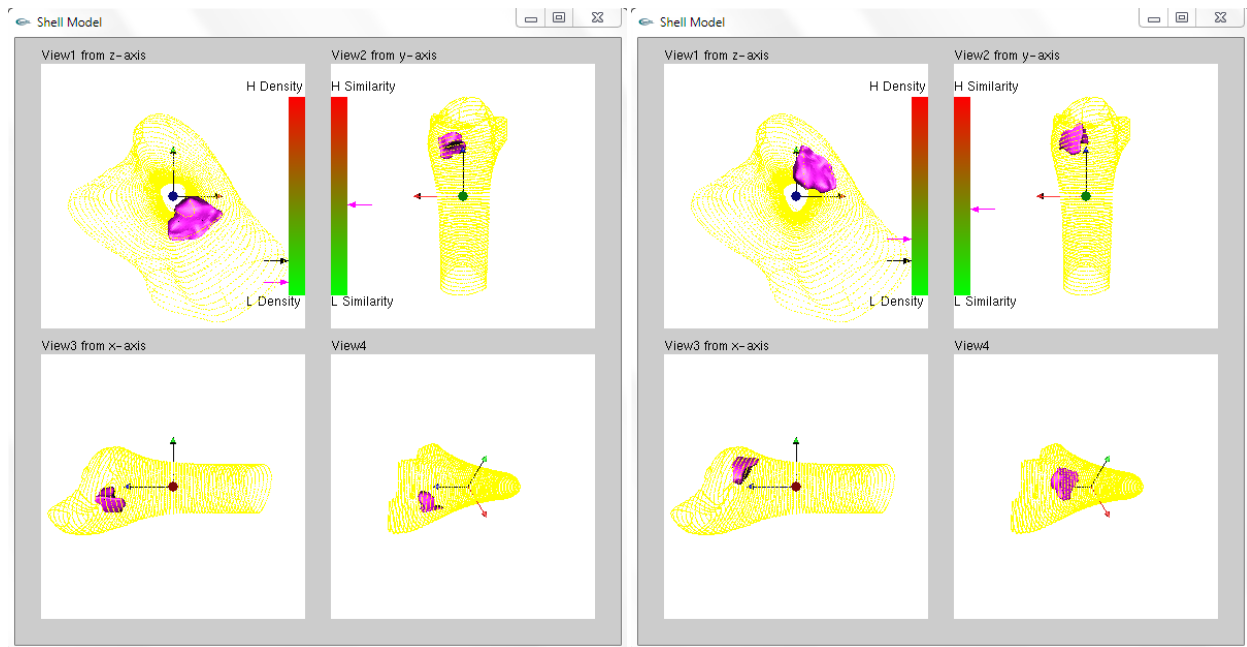


Figure 13. A *Matryoshka* shell model of a human tibia. (a) Shell 1 (210HU); (b) Shell 2 (350HU); (c) Shell 3(HU500); (d) Shell 4(850HU); (5) Shell 5(1500HU).

It is worth noting that there are two goals in the implementation, or at least, two modes of use envisioned. Although the methods in this paper allow direct investigation of the total numerical scores and optimization, surgeons may in fact desire a tool to manipulate implant sites by hand so as to receive a real-time score for each provisional harvest position. Conceptually this would take the form of an “applause meter,” which gives the surgeon feedback during manipulation of the implant in the design space. Based on this second implementation concept, an initial interactive graphics software interface has been developed (Figure 14). In this example, after aligning the ends of patient bone and donor bone, the implant was translated into the donor bone, where the initial *Density* score and *Similarity* score of the harvested implant in the donor bone were found to be 339 HU and 1, respectively. In Figure 14(a), the black arrow pointing to the left color bar shows the *Density* score of the implant in the original patient bone,



(a)

(b)

Figure 14. Implementation results for two provisional implant harvest sites. (a) Initial location of the implant within the donor bone; (b) The location of the implant is updated by rotating about the Z-axis by  $103.5^\circ$ , translating along the Z-axis direction by  $-4.0$  mm, and moving radially by  $1.0$  mm.

while the pink arrow pointing to the right color bar shows the *Density* score of the harvested implant from within the donor bone. Likewise, the pink arrow pointing to the right color bar represents the *Similarity* score (There is obviously no “original” similarity to compare against). After rotating the implant about the Z-axis by  $103^\circ$ , translating the implant along the Z-axis direction by  $-4.0$  mm, and moving the implant radially by  $1.0$  mm, the updated *Density* score and *Similarity* scores of the harvested implant in the donor bone are  $533$  HU and  $1$ , respectively. In Figure 14(b), we note that the pink arrow

pointing to the *Density* bar jumps above the black arrow, which denotes that the new provisional harvested location has a higher *Density* score than the original implant within the patient bone. In this case, the *Similarity* score remained essentially the same.

We envision a surgeon using an interactive tool to move the implant around the donor bone and monitor the *Density* and *Sensitivity* bars to aid in finding a best site for harvesting. The ideal for the allograft in most instances would be to replicate the normal native local density distribution of bone at the recipient site. However, the program would also allow the requesting surgeon to over-ride that default condition, by prescribing a desired density distribution of his/her choosing as clinical indications dictate. Under cursor control, the tissue bank operator would then provisionally position the idealized allograft geometry at a plausibly acceptable location within the donor bone geometry. Given the goodness-of-match between the provisional harvest and the idealized allograft HU distributions, and given the degree of acceptability of the structural stiffness of the corresponding provisional sacrificial supports, the overall attractiveness of that provisional harvest position would then be quantitatively scored, and feedback provided to the operator. The benefits of this new software, which would be most helpful from the clinical perspective, would be both the user-friendly real-time interface, as well as ability of the software to choose a best fit for both geometry and density. Currently available software provides no basis (other than operator judgment) for selecting the specific harvest site beyond ensuring that the implant object to be machined lies entirely within the outer surface of the donor bone. The following presents

an implementation of an automated search for a harvest location using the developed models.

To conduct an automated search for our implementation, we iterated through the design space and recorded results for *Density* and *Similarity*. Through rotations of the implant about the Z-axis by  $3^\circ$  increments, translating the implant along the Z-axis direction in 2 mm increments, and moving the implant radially by 1.5 mm increments, we generated the normalized *Density* score and *Similarity* score plots for several donor bones models. As one example, Figure 15 shows a plot of Density scoring for one sample bone, where maximal value is achieved at iteration 2575.

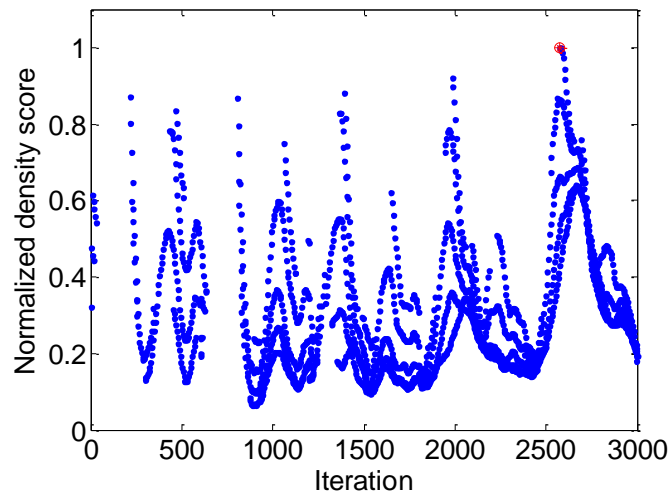


Figure 15. Plot of normalized *Density* score showing iterations about the axis, along the axis and radially.

### 3.3.2 Implant Harvesting Using CNC-RP

CNC-RP is a fully automated Subtractive Rapid Prototyping process that uses a 3-axis vertical milling machine with a 4<sup>th</sup> axis indexer for multiple setup orientations [45]. In this system, round stock material is fixed between two opposing chucks and rotated between operations using the indexer, and visibility analysis of cross sectional slice data provides a basis for automated setup planning about a single axis. This implementation uses a modified Greedy set cover algorithm to determine orientations. For each orientation, all visible surfaces are machined using simple layer-based toolpath planning while leaving a structure of “sacrificial supports” that are used to fixture the part (keeping the part attached to the remainder of the stock). The number of rotations required to machine a model is dependent upon its geometric complexity. Once all of the operations are complete, the supports are severed in a final series of operations, and the part is removed. Figure 16 illustrates the process steps for creating a typical complex part using this strategy.

The motivation for the *Matryoshka* model and harvesting search method has been to determine a solution for optimal “harvesting” when using Subtractive Rapid Prototyping (CNC-RP) for custom bone implants. To illustrate that the *Matryoshka* approach can be used to plan harvesting locations for creating a custom bone implant from a donor bone, an example of harvesting an implant using CNC-RP is demonstrated. The approach starts with scanning a potted surrogate tibia bone, as shown in Figures 17(a) and 17(b). In this instance, a laser scanner is used to create the outermost shell of the bone and pot, and then a pre-existing set of *Matryoshka* shells from a representative human tibia

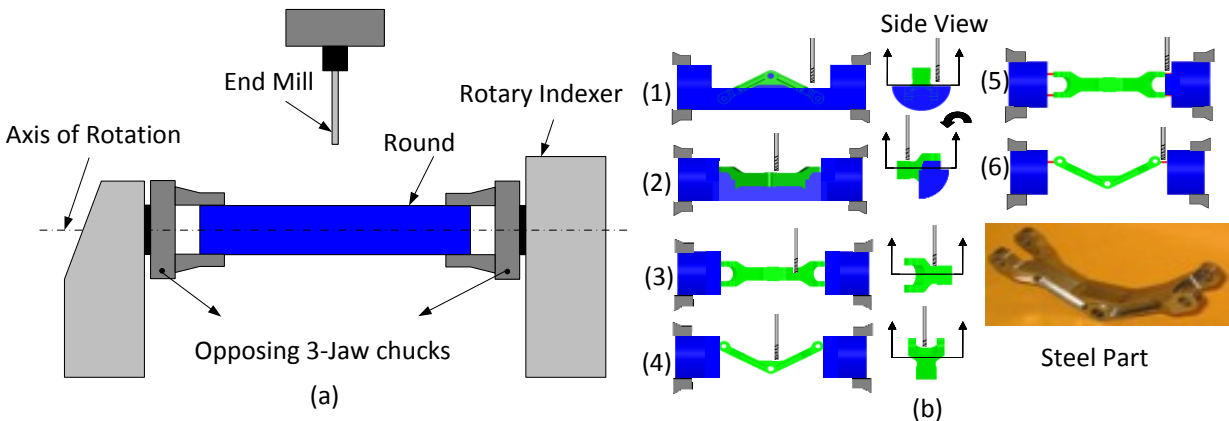


Figure 16. CNC-RP Subtractive RP process (a) CNC-RP Fixture Setup; (b) Process sequence of steps (b.1-b.4) to expose component geometry and (b.5-b.6) to expose sacrificial supports.

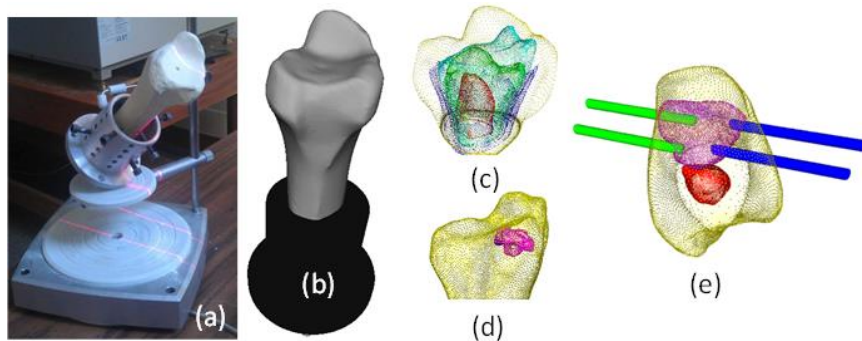


Figure 17. Pre-processing and planning for implant harvest. (a) Tibia bone in the fixture pot; (b) CAD model of scanned bone and pot; (c) *Matryoshka* shells assembled in outer shell; (d) Implant harvest site located within the bone using scoring functions; (e) Sacrificial support generation into implant geometry.

CT scan is inserted within the laser scanned shell. This step was only done in order to use a surrogate bone in the lab; the requisite CT scanning setup and approvals to scan and machine an actual bone are not in place yet. The assembled *Matryoshka* model

(17(c)) was then used to find the best position and orientation within the donor bone from which to harvest the implant, as shown in Figure 17(d) with inner shells hidden for clarity. The locations for the sacrificial supports on the implant were then automatically determined by the CNC-RP software, and are shown in Figure 17(e).

Next, a newly developed 5-axis device is used to allow the potted Tibia to be transferred as “stock” material to the CNC-RP setup. Given an implant shape in its desired position in the donor bone, the essential problem is to position the actual donor bone in such a manner that sacrificial supports can be passed in appropriate orientations through the donor bone, terminating at locations that will be just inside the to-be-harvested implant. The setup used for this purpose is shown in Figure 18. In this system, the potted donor bone is temporarily mounted to the rotary fixture and then rotated and translated to an orientation and location between two disk templates - Figure 18(a). Then, a desired number (minimum of two per disk) of the sacrificial supports can be passed through the disks so as to intersect the desired implant surfaces and then the section of bone is severed from the potted end - Figure 18(b). After drilling holes and embedding the sacrificial supports (in this setup, stainless steel screws) to the necessary depths, the bone, disks, and support units are removed *en bloc* from the fixture and mounted within the 4-axis mill chucks. Finally, the implant geometry is revealed through layerbased machining using CNC-RP developed process plans - Figure 18(c). The original implant CAD model and machined implant with supports removed are shown in Figures 18(d) and (e).

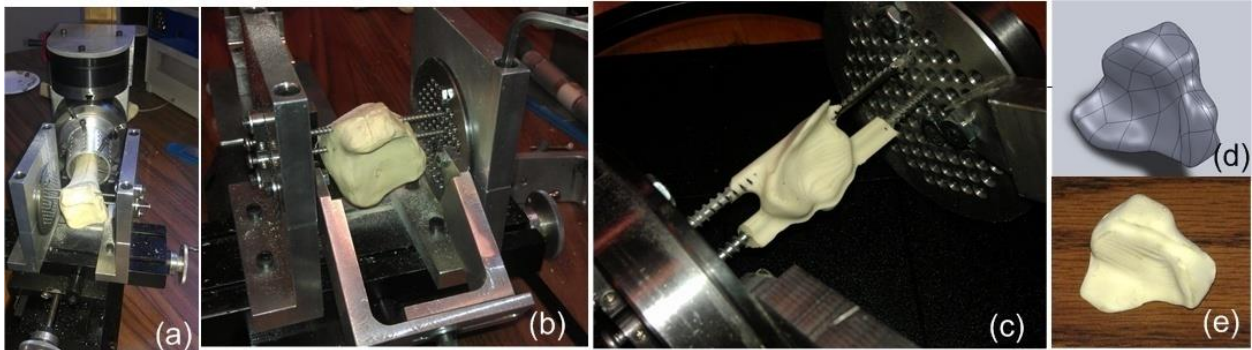


Figure 18. Implant harvesting using CNC-RP. (a) 5-axis positioning device places the tibia bone surrogate between the disks; (b) Support-screw-affixed and then severed section of the bone prepared for transfer to mill; (c) Nearly complete machined implant; (d) Original implant CAD model; (e) Final implant with supports removed.

Complete processing of an implant can be done in a matter of hours. As presently implemented, the harvest site search process takes approximately 20 minutes. The SRP software requires approximately 15-30 minutes to automatically generate all setups, supports, and toolpaths. Finally, the total processing time using CNC-RP is on the order of a few hours. This overall time period is consistent with the goal of delivering a custom implant within a few days of a traumatic incident; most surgeries for extreme trauma involve waiting several days for physiologic stabilization, reduction in swelling, etc.

### 3.4 Conclusion

This paper presents a new method for multi-material model representation using nested polygonal shells, analogous to a *Matryoshka* doll. Compared with methods of hand-creating an assembly model for input to a multi-material additive RP system, this

method could potentially be completely automated, given a set of parameters. This work illustrates how the *Matryoshka* model can be used to plan harvesting locations for creating custom bone implants from within actual human donor bones, and it develops an approach to calculate a *Density* score and *Similarity* score for an arbitrary provisional implant harvest site, to evaluate the overall effectiveness of that harvest site.

This approach to finding the optimal implant harvest site within a donor bone still leaves room for improvement, and is not necessarily a generic solution for all multi-material components. The method has, however, proven effective for human long bones, which can be approximated by a cylinder model. In these bones, it is relatively easy to find the center line, and it is reasonable to assume that the density of the long bone decreases from the outer surface to the center line. Based on this assumption, the implant is simply rotated around the center line. If the bone is not a long bone, and/or cannot be approximated as a cylinder, one would need to allow the implant to “tumble” in 3D space. Hence, an exhaustive search would probably not be tractable since the solution space would be much larger. Future work with the *Matryoshka* approach could be used to develop a better harvesting solution for irregular and/or flat bones. It could also be used to pursue variants of the method for use in industrial components which may have less amorphous shapes, and which could be printed using existing additive systems such as LENS or polyjet printing.

### **3.5 Reference**

[1] Kumar, V., Burns, D., Dutta, D. and Hoffmann, C., A framework for object modeling, *Computer-Aided Design*, 1999, 31(9), 541-556.

- [2] Markworth, A.J., Ramesh, K.S. and Parks, W.P., Modeling studies applied to functionally graded materials, *Journal of Materials Science*, 1995, 30(9), 2183-2193.
- [3] Kruth, J.P., Mercelis, P., Vaerenbergh, J.V., Froyen, L. and Rombouts, M., Binding mechanisms in selective laser sintering and selective laser melting, *Rapid Prototyping Journal*, 2005, 11(1), 26-36.
- [4] Harrysson, O.L.A., Cansizoglu, O., Marcellin-Little, D.J., Cormier, D.R. and West, H.A., Direct metal fabrication of titanium implants with tailored materials and mechanical properties using electron beam melting technology, *Materials Science & Engineering. C, Biomimetic Materials, sensors and systems*, 2008, 28(3), 366-373.
- [5] Thomsen, P., Malmström, J., Emanuelsson, L., René, M. and Snis, A., Electron beam-melted, free-form fabricated titanium alloy implants: material surface characterization and early bone response in rabbits, *Journal of Biomedical Materials Research Part B Applied Biomaterials*, 2009, 90(1), 35-44.
- [6] España, F.A., Balla, V.K., Bose, S. and Bandyopadhyay, A., Design and fabrication of CoCrMo alloy based novel structures for load bearing implants using laser engineered net shaping, *Materials Science and Engineering: C*, 2009, 30(1), 50-57.
- [7] Bandyopadhyay, A., Krishna, B.V., Xue, W. and Bose, S., Application of Laser Engineered Net Shaping (LENS) to manufacture porous and functionally graded structures for load bearing implants, *Journal of Materials Science: Materials in Medicine*, 2009, 20(1), 29-34.
- [8] Balla, V.K., Bodhak, S., Bose, S. and Bandyopadhyay, A., Porous tantalum structures for bone Implants: fabrication, mechanical and in vitro biological properties, *Acta Biomater*, 2010, 6(8), 3349-3359.
- [9] Williams, C.B., Mistree, F.M. and Rosen, D.W., Investigation of solid freeform fabrication processes for the manufacture of parts with designed mesostructure, ASME IDETC Design for Manufacturing and the Life Cycle Conference, 2005.
- [10] Wang, H., Johnston, S.R. and Rosen, D.W., Design of a graded cellular structure for an acetabular hip replacement component, The Seventeenth Solid Freeform Fabrication Symposium, 2006, 111-123.
- [11] Kou, X.Y. and Tan, S.T., Heterogeneous object modeling: a review, *Computer-Aided Design*, 2007, 39(4), 284-301.
- [12] Chen, M. and Tucker, J.V., Constructive volume geometry, *Computer Graphics Forum*, 2000, 19(4), 281-293.

- [13] Chandru, V., Manohar, S. and Prakash, C.E., Voxel-based modeling for layered manufacturing, *Computer Graphics and Applications, IEEE*, 1999, 15(6), 42-47.
- [14] Jackson, T., Analysis of functionally graded material object representation methods, Ph.D. thesis. Massachusetts Institute of Technology, 2000.
- [15] Shin, K.H. and Dutta, D, Constructive representation of heterogeneous objects, *Journal of Computing and Information Science in Engineering*, 2001, 1(3), 205-217.
- [16] Zhu, F., Visualized CAD modeling and layered manufacturing modeling for components made of a multiphase perfect material, M.Phil. Thesis. The University of Hong Kong, 2004.
- [17] Elishakoff, I., Gentilini, C. and Viola, E., Three-dimensional analysis of an all-round clamped plate made of functionally graded materials, *Acta Mechanica*, 2005, 180(1-4), 21-36.
- [18] Siu, Y.K. and Tan, S.T., Source-based heterogeneous solid modeling, *Computer-Aided Design*, 2002, 34(1), 41-55.
- [19] Biswas, A., Shapiro, V. and Tsukanov, I., Heterogeneous material modeling with distance fields, *Computer Aided Geometric Design*, 2004, 21(3), 215-242.
- [20] Liu, H., Maekawa, T., Patrikalakis, N.M., Sachs, E.M. and Cho, W., Methods for feature-based design of heterogeneous solids, *Computer-Aided Design*, 2004, 36(12), 1141-1159.
- [21] Samanta, K. and Koc, B., Feature-based design and material blending for freeform heterogeneous object modeling, *Computer-Aided Design*, 2005, 37(3), 287-305.
- [22] Qian, X. and Dutta, D., Design of heterogeneous turbine blade, *Computer-Aided Design*, 2003, 35(3), 319-329.
- [23] Pasko, A., Adzhiev, V., Schmitt, B. and Schlick, C., Constructive hyper volume modeling, *Graphical Models*, 2001, 63(6), 413-442.
- [24] Yao, J. and Taylor, R., Construction and simplification of bone density models, *Proceedings of SPIE*, 2001, 4322, 814-823.
- [25] Bibb, R. and Sias, G., Bone structure models using Stereolithography: a technical note, *Rapid Prototyping Journal*, 2002, 8(1), 25-29.
- [26] Chen, Z.Z., Li, D.C., Lu, B.H., Tang, Y.P., Sun, M.L. and Wang, Z., Fabrication of artificial bioactive bone using rapid prototyping, *Rapid Prototyping Journal*, 2004, 10(5), 327-333.

- [27] Fang, Z.-B., Starly, B., Shokoufandeh, A., Regli, W. and Sun, W., A computer-aided multi-scale modeling and direct fabrication of bone structure, *Computer-Aided Design and Applications*, 2005, 2(5), 627-634.
- [28] Sun, W., Starly, B., Darling, A. and Gomez, C., Computer-aided tissue engineering: application to biomimetic modeling and design of tissue scaffolds, *Biotechnology and Applied Biochemistry*, 2004, 39(1), 49-58.
- [29] <http://academic.uofs.edu/faculty/kosmahle1/courses/pt245/trabecul.htm> (accessed October 20<sup>th</sup> 2012).
- [30] Nauth A, McKee M.D., Einhorn T.A., Watson J.T., Li R. and Schemitsch E.H., Managing bone defects, *J Orthop Trauma*, 2011, 25(8), 462-466.
- [31] Bosse M.J., MacKenzie E.J., Kellam J.F., Burgess A.R., Webb L.X., Swiontkowski M.F., Sanders R.W., Jones A.L., McAndrew M.P., Patterson B.M., McCarthy M.L., Trivison T.G. and Castillo R.C., An analysis of outcomes of reconstruction or amputation after leg-threatening injuries, *New Engl J Med.*, 2002, 347(24),1924-1931.
- [32] Vallier, H. A., Hennessey, T. A., Sontich, J. K., & Patterson, B. M., Failure of LCP condylar plate fixation in the distal part of the femur - A report of six cases. *The Journal of Bone & Joint Surgery Case Connector*, 2006, 88(4), 846-853.
- [33] Skendzel, J. G., & Sekiya, J. K., Arthroscopic glenoid osteochondral allograft reconstruction without subscapularis takedown: technique and literature review. *Arthroscopy: The Journal of Arthroscopic & Related Surgery*, 2011, 27(1), 129-135.
- [34] Clowers, B. E., and Myerson, M. S. (2011). A novel surgical technique for the management of massive osseous defects in the hindfoot with bulk allograft, *Foot and ankle clinics*, 2011, 16(1), 181-189.
- [35] <http://www.thefoxisblack.com/2009/12/07/matte-black-nesting-dolls-by-muji/>  
(accessed September 1<sup>st</sup> 2012).
- [36] <http://geekopedia.blogspot.com/2009/04/munecas-rusas.html>  
(accessed September 1<sup>st</sup> 2012).
- [37] Frank, M.C., Hunt, C.V., Anderson, D.D., McKinley, T.O., and Brown, T.D., Rapid manufacturing in biomedical materials: using subtractive rapid prototyping for bone replacement, *Proceedings of the Solid Freeform Fabrication Symposium*, 2008, 686-696.

- [38] Frank, M.C., Wysk, R.A. and Joshi, S.B., Determining setup orientations from the visibility of slice geometry for rapid CNC machining, *Journal of Manufacturing Science and Engineering*, 2006, 128(1), 228-238.
- [39] Li, Y. and Frank, M.C., Machinability analysis for 3-axis flat end milling, *Journal of Manufacturing Science and Engineering, Transactions of the ASME*, 2006, 128(2), 454-464.
- [40] Li, Y. and Frank, M.C., Computing non-visibility of convex polygonal facets on the surface of a polyhedral CAD model, *Computer-Aided Design*, 2007, 39(9), 732-744.
- [41] Frank, M.C., Implementing rapid prototyping using CNC machining (CNC-RP) through a CAD/CAM interface, Proceedings of the Solid Freeform Fabrication Symposium, 2007, 112-123.
- [42] Boonsuk, W. and Frank, M.C., Automated fixture design for a rapid machining process, *Rapid Prototyping Journal*, 2009, 15(2), 111-125.
- [43] Petrzela, E.J. and Frank, M.C., Advanced process planning for subtractive rapid prototyping, *Rapid Prototyping Journal*, 2010, 16(3), 216-224.
- [44] Thomas T.P., Anderson, D.D., Willis, A.R., Liu, P., Marsh, J.L, and Brown, T.D., Virtual pre-operative reconstruction planning for comminuted articular fractures, *Clinical Biomechanics*, 2011, 26(2), 109-115.
- [45] Frank, M.C., Wysk, R.A., and Joshi, S.B., Rapid Planning for CNC Machining - A New Approach to Rapid Prototyping, *Journal of Manufacturing Systems, SME*, 2004, 23(3), 242-255.

## **CHAPTER 4. AUTOMATED FIXTURE DESIGN FOR THE SUBTRACTIVE RAPID MACHINING OF HETEROGENEOUS MATERIALS: APPLICATIONS FOR NATURAL BONE IMPLANT MANUFACTURING**

A paper to be submitted to Rapid Prototyping Journal

### **Abstract**

**Purpose** - The purpose of this paper is to present a new method for the automated design of a fixturing system for the subtractive rapid machining of heterogeneous materials, namely, natural bone implants.

**Design/methodology/approach** - The proposed method employs a method derived from the idea of sacrificial supports in order to support a rapid machined bone implant which is harvested within a donor bone. The parameters depth, diameter, and location of the sacrificial supports depend on the different distributions of materials in the part. During the machining process, the material around the embedded sacrificial supports is machined, and at the end of the process, only the supports are connected to the part and the remaining fixture disks.

**Findings** - The sacrificial support design approach provides a feasible solution for use with heterogeneous materials for use in a subtractive rapid prototyping process.

**Originality/Value** – This work is the first to address a unique application of rapid technologies for harvesting custom implants from donated allograft bone. It considers

the further challenge of dealing with a material density distribution across the interior of the bone.

**Keywords** - Rapid prototyping, rapid manufacturing, automated fixturing, bone implants.

#### 4.1 Introduction

Fixtures are used to hold, secure and support a part in the correct orientation during a manufacturing process. Traditional fixturing techniques use a number of workpiece holding elements such as vises, clamps, V-block, modular plates, etc. depending on the product variety and volume. Proper fixture design can dramatically reduce the manufacturing cost, the labor skill requirements, etc. [1]. Over the past decades, fixture design has garnered attention due to the extreme diversity and complexity of new part designs [2]. Arguably, the best success story for automated fixturing is owed to the field of Additive Manufacturing (AM), where sacrificial supports are automatically generated very quickly and robustly; immediately prior to the start of processing [3].

Existing RP&M techniques actually fall into three categories: additive, subtractive or hybrid additive/subtractive processes. In most current additive processes, the fixtures used to hold the part are called *sacrificial* support structures, which are automatically added during the building process for supporting the overhanging features of the part and are then eliminated in the post-processing step. In general though, the idea of sacrificial supports can be divided into two basic categories: *passive* sacrificial supports and *active* sacrificial supports. Passive sacrificial supports are those that emerge on

their own, generally, in the form of un-fused powders, such as those found in Selective Laser Sintering (SLS) and 3D Printing (3DP) [4, 5]. In other methods, the supports have been actively designed as such, for example those used in Stereolithography (SLA), and Fused Deposition Modeling (FDM) [6-9]. In either case, the supports are not really designed by the user, generally, rather the process planning software handles their design based on each unique part automatically.

Heterogeneous material, in general, refers to objects with spatially different material compositions or structures [10, 11]. Heterogeneous objects are mainly classified into two groups, multi-material objects, which have distinct material domains and functionally graded materials (FGMs), which have continuous material variation in composition and structure gradually over volume. Some existing additive manufacturing (AM) techniques including 3D printing, Laser Engineered Net Shaping (LENS) and PolyJet Technologies, can make parts with multiple materials, or at least designate multiple components in color (3DP). In particular, the multi-material 3D printing system “Connex” developed by Objet Ltd. has the capability of printing parts made from over a dozen materials [12] in a single print. Though a wide range of homogeneous and heterogeneous material mixtures have been employed in additive manufacturing, there is still a need for developing additional materials [13, 14]. Moreover, many of the materials commonly used in additive RP manufacturing processes such as resins and powders cannot be used for fabricating truly functional models based on the designed part specifications [3].

In order to improve the variety of materials available, Subtractive Rapid Prototyping has been developed in an effort to produce functional prototypes using appropriate materials, at least for a smaller subset of part geometries. CNC-RP is a subtractive process that can create functional 3D parts from a wide variety of machinable materials [15, 16]. As opposed to additive processes, the CNC-RP process involves sequentially removing material (CNC machining) from bar stock to create complex geometric shapes. Instead of adding support material as in AM, CNC-RP supports are created as small features added to the solid model geometry (i.e. cylinders) and incrementally created during the machining process along with other part features. When the machining process is finished, only these sacrificial entities are connecting the part to the stock material.

The machining setups for the CNC-RP process are shown in Figure 1. In this case, a component is being machined using sacrificial supports to retain the part at its ends along the axis of rotation. Four supports are used as shown in Figure 1(b), and 4 orientations are needed to machine the stock and create all the visible surface and supports as shown in Figure 1(b.1-b.4). By the end of machining process, only two permanent supports need to remain, as shown in Figure 1(b.5). Lastly, the part is cut from the stock by sawing the two remaining supports, as shown in Figure 1(b.6). The automated CNC-RP machining process as described above was originally developed for making industrial parts from homogeneous materials, especially in solid metal.

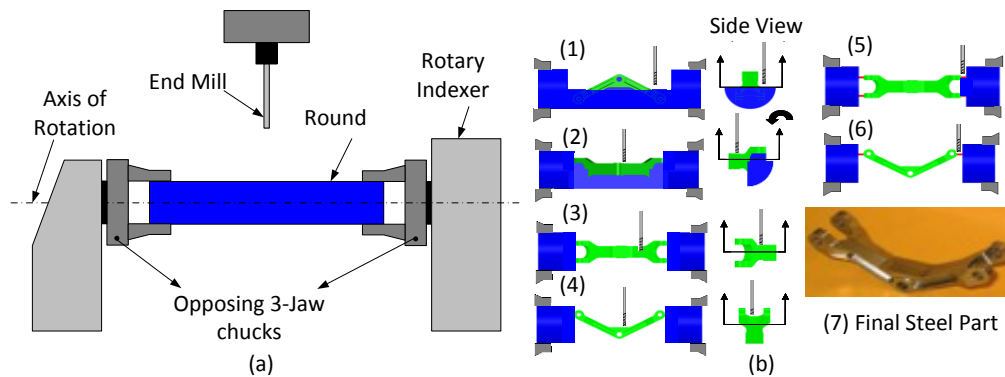


Figure 1. CNC-RP process. (a) Rotary fixture setup; (b) Process sequence of steps (b.1-b.4) to expose component geometry and (b.5-b.6) to expose sacrificial supports.

However, if a part is to be made of heterogeneous materials, it adds a significant new challenge for support design. One particularly challenging heterogeneous materials is natural bone, which has a density distribution from inside to outside that spans a significant range. To illustrate, Figure 2

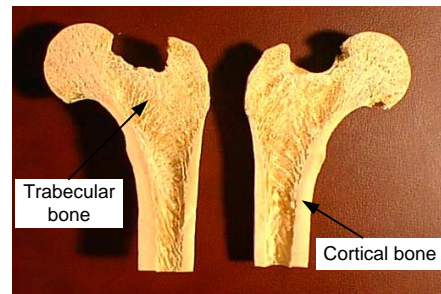


Figure 2. A cross-sectional view of a femur bone [17]

shows a cross sectional view of a femur bone, showing the spongy, low density trabecular bone in the middle, versus the high-density cortical bone on the outside. Bone is a very important material for its use in reconstructive surgery in the form of bone implants or *grafts*. Bone implants or *grafts* are widely used in the treatment of missing pieces of bone in cases of trauma and other bone loss. In order for the human body to accept the bone implant material and heal properly, it is essential that the bone implant should be both mechanically and biologically compatible. A surgical bone implant might call for a bone material density

that is highly, or almost all cortical bone, or may call for some distribution of densities, or simply try to match the general gradient directions in density of the surrounding bone. In any case, there arises the challenge of having correctly shaped implants created from appropriate material. A newly specialized variant of CNC-RP has been developed to meet this unique challenge.

Figure 3 illustrates the machining setup with one axis of rotation used in the new CNC-RP<sub>bio</sub> process. In this work, a “potted” bone is temporarily mounted to a rotary fixture and then rotated and translated to an orientation and location between two fixture disk templates (Figure 3a). The bone is potted, or fixture in a mechanical holding pot with a set of compression screws in order to create a known coordinate system for an arbitrary shape like a bone. Then, a number of sacrificial supports can be passed through the disks so as to embed into the desired implant surfaces. Specifically, a set of surgical screws are inserted through the disks into the bone, terminating where the implant *will* exist upon completion. After screwing in the supports, the bone is cut along its shaft and now can serve as the “stock material” (Figure 3b). The convenient advantage to this method is that we go from a cumbersome bone shape that is a fixturing problem to a section of bone between round fixture plates; essentially replicating what CNC-RP typically uses - round bar stock between centers. All the rotations and translations of the potted bone, drill locations and depths for the supports, and even the saw cut location are provided in an automatically generated setup sheet. Once fixture between the disks, the entire construct is moved from this offline fixture and mounted within the 4-axis mill chucks. During the subsequent machining process, the stock is rotated several times

about the axis of rotation until all surfaces are completed machined, as shown in Figure 3(c). Finally, the supports are removed (Figure 3e) to release the custom machined bone implant.

The CNC-RP<sub>bio</sub> machining process has the ability to calculate the visibility for polyhedral CAD models to determine the machining rotation axis and then calculate the minimum number of the setup orientations required to create the part about the rotation axis, as was done in the past. One unique challenge is to develop algorithms for automated support generation in this new application.

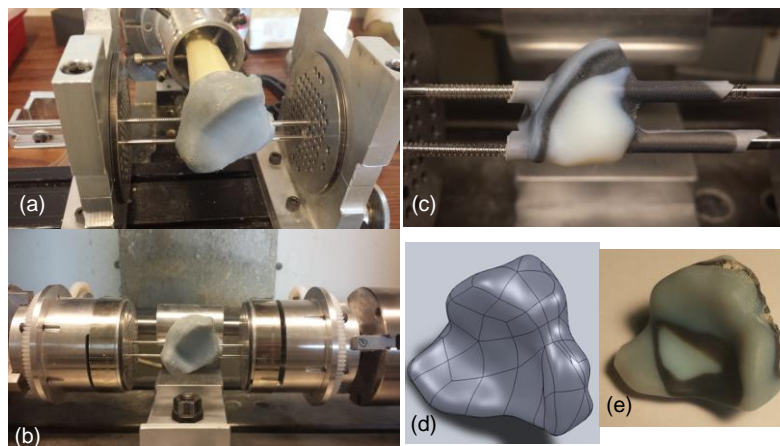


Figure 3. Implant harvesting using CNC-RP<sub>bio</sub>. (a) 5-axis positioning device places a potted tibia bone surrogate between the disks; (b) It is support-screw-affixed and then severed section of the bone is prepared for transfer to mill; (c) Nearly complete machined implant; (d) CAD model of the implant; (e) Final implant with supports removed.

This paper presents an approach to determine a feasible layout of the sacrificial support screws for a free-form shape part (bone implant) within a heterogeneous density distribution (natural bone stock material and shape). The goal of this work is to automatically generate an arbitrary free-form shaped object from within another arbitrary free-form shaped stock object, where each has a unique material density distribution, and to create these “parts” at the push of a button. If successful, we could enable the cost effective manufacturing of bio-compatible implants that are custom shaped to the unique needs of a patient, without the hand-sculpting of a surgeon.

#### **4.2 Related Work**

Fixture design techniques involve providing proper part orientation, location, support, and clamping such that all the model features can ultimately be machined. Traditional fixturing techniques using clamps, vices, V-blocks, modular plates, etc. have some disadvantages such as reduced reachability for tools and increased process planning and setup time. Therefore, improvement in fixturing and fixture design can result in significantly improved accuracy of machined parts, time savings and other benefits. As a result, great attention has been directed towards the development of flexible fixture systems in the past decades [2, 18].

Since their inception in the 1980s rapid prototyping processes were intended to be push-button, resulting in considerable research to address fixture designs in conjunction with layer slicing and planning. For example, Ajay and Joneja [19] developed an integrated software system called Quick turnaround cell (QTC) for rapid prototyping.

This fixture system was capable of machining prismatic parts but did not provide a feasible fixture solution for arbitrary part shapes. Tseng proposed [20] a feature-based fixturing analysis method to analyze the parameters required for the intermediate steps in a successive feature-based machining process. The output of the fixturing parameters included locating faces, clamping points and feasible height. However, the shape of parts was restricted to prismatic or otherwise feature-based designs. Gandhi et al. [21, 22] proposed a fluidized bed technique as a flexible fixturing process. It utilizes materials that can change from a solid phase to a liquid phase and vice versa. When the material is in the liquid state, the fixturing medium could accommodate a wide variety of different part geometries. Choi [23] developed a reference-free part encapsulation (RFPE) system that could fixture arbitrary geometric shapes during machining. The basic concept involves filling the space around the part with low melting point material, allowing to solidify, then machining, re-melting and re-orienting for the next step, etc. After all machining was completed, the filler material is finally melted away to reveal the finished part. Shin et al. [24] proposed a new type of technology using a combination of high-speed machining technology and an automatic fixturing process. It also used low-melting-point metal alloys to hold the workpiece during multi-face machining. However, these processes cause thermal shrink and expansion problems and were cumbersome to use. DeskProto software [25] uses a rotary axis and support tabs to hold the part during the machining, somewhat similar to CNC-RP; however, it does not provide analysis about the support design to determine if it is a feasible solution for any arbitrary part. Roland [26] uses a similar fixture approach to Deskproto, with support tabs that are added to the part, but it also does not give an

optimized or validated design to show the support works for any free-form parts. Boonsuk et al. [27] developed an automated fixture design for CNC-RP, which includes the design of sacrificial support length, shape, size, number, and location to minimize allowable deflection of the part while maximizing machinable surface area. However, in this sacrificial design, it assumes the part is made of one homogeneous material. The automated support generation approach for mask image projection based additive manufacturing developed by Zhou et al. [28] provided a scientific foundation for just generating sufficient supports for arbitrary geometries. This method was incorporated by EnvisionTec in its Perfactory RP software system [29]. Although numerous methods have been investigated in the field of rapid technologies, there is no effective solution for a subtractive rapid manufacturing process with heterogeneous materials in the literature.

### **4.3 Overview of Sacrificial Support Generation for a Bone Implant**

In this section, we provide an overview of designing the sacrificial support structure from a set of nested STL shells, called the *Matryoshka* Model [30]. In this work a *Matryoshka* shell model is used to describe density distribution of the bone. The *Matryoshka* model is generated via an iterative process of thresholding the Hounsfield Unit (HU) data from a computed tomography (CT) scan, thereby delineating regions of progressively increasing bone density. An example of a *Matryoshka* model for the human tibia is shown in Figure 4. This model was constructed of five shells: an innermost medullary cavity shell (Shell 1), a low-density cancellous bone shell (Shell 2), a high-density cancellous bone shell (Shell 3), a cortical bone shell (Shell 4), and a bone outer surface

(Shell 5). In this manner, the entire 3D volume of the bone is classified as being within one of four bone regions, bounded by five shells. The thresholding HU used to generate the shells will be discussed in the support layout section.

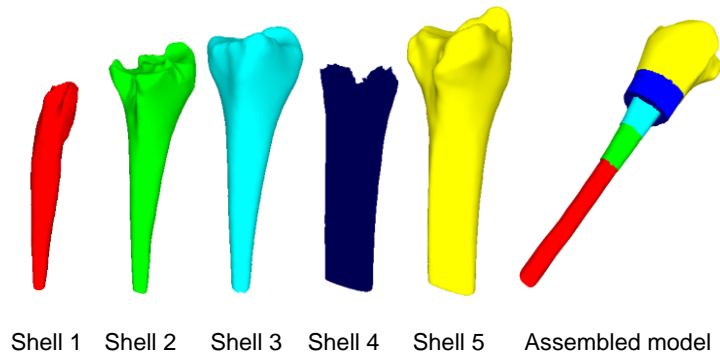


Figure 4. *Matryoshka* model of the human tibia. From left to right: five shells generated from the medullary canal to outer bony surface, along with a cut-away view of an assembled final model.

Next, a harvesting algorithm is used to identify the best location to create the implant from within the tibia bone (donor bone), based on the given geometries and density distributions. For example, a selected harvest location within a donor bone is illustrated in Figure 5a. As discussed previously, after severing from the donor bone, only a bone cut section serves as the “stock material” between fixture disks; which is clamped in the CNC mill between rotary chucks. The rotation axis is already determined and all the supports are parallel to the axis of rotation. One end of the supports will be embedded into the stock (bone) and the other end of the supports is attached to the designed fixture disk. The sacrificial supports are considered as new CAD features added to the solid part model. Therefore, the process planning will include generating the tool paths

on the support features as well as the part model; making the cutting tool avoid collision with the support screws.

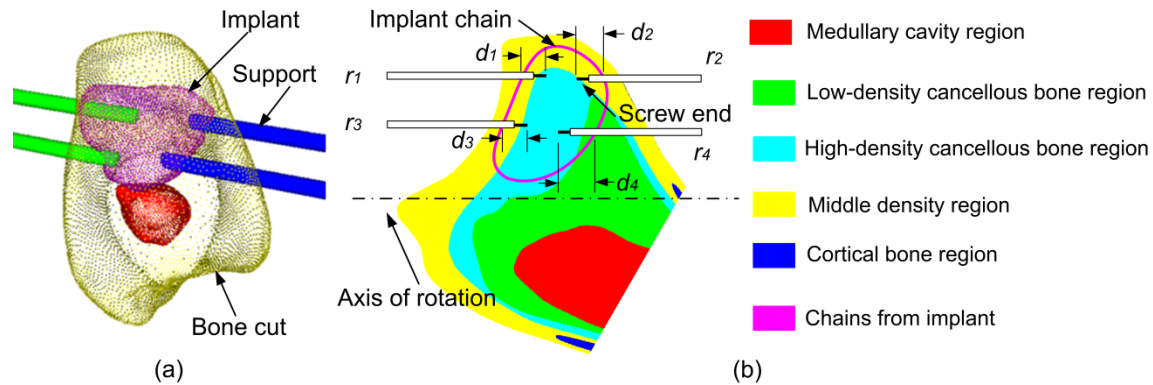


Figure 5. (a) Sacrificial support generation into implant geometry; (b) Support design parameters: depth ( $d_1, d_2, d_3, d_4$ ), size ( $r_1, r_2, r_3, r_4$ ), and location of supports.

Currently, surgical screws (titanium, stainless steel, bioabsorbable materials, etc) are used for internal fixation of bones. In this work, stainless surgical screws are chosen as sacrificial supports to provide fixation during the machining process. To place these screws, the technician first drills screw holes in the bone to accommodate a screw for rigid fixation. The propensity for crack initiation and propagation throughout the implant generally increases due to the weakening of material around the screws during the insertion. To reduce the stresses generated by the screw insertion, a proper size of drill hole is needed; undersized drill bits from the manufacturers' specifications are utilized.

The research challenge is to develop a method to automatically determine where, and how deep and with what diameter screws should one fixture the implant. The objective is to reduce the stresses from machining forces, while enabling complete geometry

creation, and limiting the depth with which the screw holes need to be drilled. The design parameters of the support can therefore be summarized by depth, size, shape and location (Figure 5(a)). These parameters are critical because the cutting force of the machining process will result in a certain amount of VonMises stress in the bone material. In addition to reducing stress, we also want to minimize the embedded support depth within the implant. In this implementation, a safety factor of 2 is employed, such that the VonMises stress must be less than 50 percent of the compressive strength of the implant material [31, 32]. However, the design of each support parameter is not an independent problem. For example, increasing the support diameter would reduce the VonMises stress caused by the cutting force, but that would result in more surface geometry on the part becoming non-machinable and leaving subsequently larger holes in the implant. In this research, we use finite element analysis (FEA) to design and optimize the support structure to meet those challenges. The following sections describe the design of these support parameters.

### ***Depth of the sacrificial support***

During machining, the main strain caused by the cutting force is compressive strain. When cutting forces are applied to the bone, it results in VonMises stress on the contact surface between the surgical screws and the bone. The VonMises stress is expressed as:

$$\sigma_{VonMises} = \sqrt{\frac{(\sigma_1 - \sigma_2)^2 + (\sigma_2 - \sigma_3)^2 + (\sigma_3 - \sigma_1)^2}{2}}, \quad (1)$$

$$\sigma_{1,2} = \frac{\sigma_x + \sigma_y}{2} \pm \sqrt{\left(\frac{\sigma_x - \sigma_y}{2}\right)^2 + \tau_{xy}^2}, \quad (2)$$

Where  $\sigma_1, \sigma_2, \sigma_3$  are principal stress,  $\tau_{xy}$  is the shear stress, and  $\sigma_x, \sigma_y$  are normal stress in x and y direction, respectively.

The compressive strength is the capacity of a material or structure to withstand loads tending to reduce size. The relationship between the ultimate strength and bone density can be described as [33]:

$$S = S_c \left(\dot{\varepsilon}\right)^{0.06} \left(\frac{\rho}{\rho_c}\right)^2 \quad (3)$$

Where  $S$  is the compressive strength ( $\text{MN/m}^2$ ) of a bone specimen of apparent density  $\rho$  ( $\text{g/cm}^3$ ) tested at a strain rate (loading rate) of ( $\text{sec}^{-1}$ ) and  $S_c$  is the compressive strength of the bone with density  $\rho_c$  tested at a strain rate of  $1.0 \text{ sec}^{-1}$ . Human compact bone tested at a strain rate of  $1.0 \text{ sec}^{-1}$  has a compressive strength of  $221 \text{ MN/m}^2$  and a density of approximately  $1.8 \text{ g/cm}^3$ . Using these values, equation (3) is simplified to:

$$S = 68 \left(\dot{\varepsilon}\right)^{0.06} \rho^2 \quad (4)$$

Considering steel has a tensile strength range from approximately 300 MPa to more than 1882 MPa, depending on the type of alloy. Since bone's strength is significantly less, it should be easier to machine than steel. The typical feedrate which is used to machine aluminum and steel in the ISU lab is around 10ipm. For a conservative approach, the same feedrate could be applied to the machining of human bone. Hence,

the loading rate of bone can be approximated to be  $4.83 \text{ /sec}^{-1}$ . By substituting this loading rate into equation (4), the bone ultimate strength equation can be expressed as:

$$S = 74.7363\rho^2 \quad (5)$$

The bone density is in linear relationship with Hounsfield Unit (HU) data from a computed tomography (CT) scan. It is assumed that the HU value for water is 0 and the maximum bone HU value for the tibia bone model used in this paper is 1500. The approximate maximal apparent density of bone is  $2.0\text{g/cm}^3$ . Thus, the bone density is represented as:

$$\rho = 2.0 \frac{HU}{1500} \quad (6)$$

Obviously, the deeper the support screw is embedded, the larger the hole that will remain after removal. Hence, selecting an optimal depth of the support needs to consider both the density distribution of the part and the ultimate compressive strength of the material; example given in Figure 6. The design of the supports shown on the right side in Figure 6(a) are located in low-density cancellous bone regions based on the consideration that the supports should go less deep into the bone implant ( $d_2$  and  $d_4$ ). In Figure 6(b) the depth of supports 2 and 4 increase until they reach the high-density cancellous bone region ( $d_2$  and  $d_4$ ). The support design in Figure 6(a) will result in small holes in the implant compared with the support layout shown in Figure 6(b). However, for the support layout shown in Figure 6(a), the material in low density cancellous bone region usually has a low compressive strength. Therefore, if the VonMises stress at the

ends of the supports 2 and 4 is greater than the material compressive strength, the supports could cause failure (cracking) of the bone material during machining.

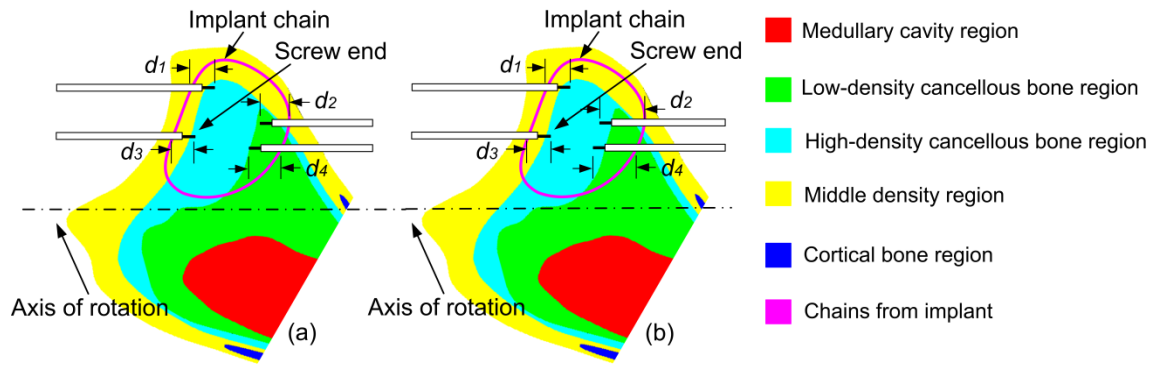


Figure 6. Support design with small depth (a) and large depth (b).

### ***Shape of the sacrificial support***

Sacrificial supports could be created in any shape such as circles, squares, ellipses, or rectangles. However, for the convenience of drilling holes into the part, a cylindrical shape is chosen in the current implementation. In CNC-RP<sub>bio</sub>, the CAD model (STL file) of the part is sliced into cross sections for analysis and process planning. Since a slice file is used, the contour of the slice is offset inwardly by more than the radius of the screws to provide a feasible location to put the support center. Figure 7 shows the offset contour of an implant cross sectional slice.

Feasible region for locating center of cylindrical support

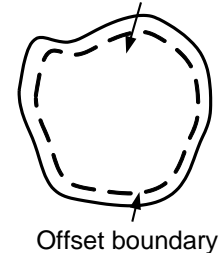


Figure 7. Offset contour.

### ***Number of sacrificial supports***

The machinable surface area decreases as the number of sacrificial support increases, since the presence of a support (surgical screw in this case) serve to obstruct access of the machine tool to the implant surfaces. Hence, additional orientations could be needed if the accessibility of the tool is blocked by additional supports. However, we only use one screw on each end; for example, the part will undergo significant twisting when the cutting force is applied. To simplify this problem, the support design used is simply be 2:2 (#supports on each end along axis). Figure 8(a) shows tool accessibility when two supports are used. The accessible angle ( $2\theta$ ) is expressed as:

$$2\theta = 2 \cos^{-1} \left( \frac{D_t + 2r}{D} \right), \quad (7)$$

Where,  $D_t$  is the diameter of the tool,  $D$  is the distance between the center of the two supports on the end, and  $r$  is the radius of the supports. Consider  $D = k (D_t + 2r)$ , equation (7) becomes:

$$2\theta = 2 \cos^{-1} \left( \frac{1}{k} \right), \quad (8)$$

Since  $D_t$  and  $r$  are constants, when  $k$  increases, the distance between the center of the two supports increases. From equation (8), when  $k$  increases, the accessible angle increases. Figure 8(b) illustrates the relationship between  $k$  and accessible angle. From Figure 8(b), we notice that when  $k$  increases from 1 to 2, the accessible angle increase

from  $0^\circ$  to  $120^\circ$ , therefore, the recommended distance between the center of the two supports should be at least twice of  $D_t + 2r$ .

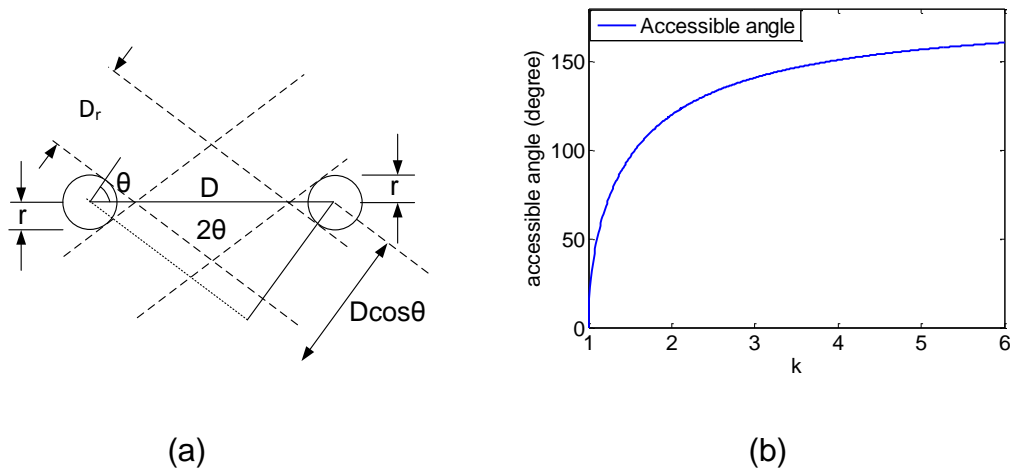


Figure 8. Accessible angle versus support distance [27].

### ***Size of the sacrificial support***

Since cylindrical supports are used in our research, the next step is to select the size (diameter) of the screws. The design of the sacrificial support size is not an independent problem, since other factors such as the support depth as well as the location of the support will affect the VonMises stress caused by the cutting force. Determining support size with other parameters gives a somewhat circular problem. For instance, increasing the diameter of the support would reduce the VonMises stress, but increasing the support diameter would change the feasible locations for the support. However, changing the support location could also affect the VonMises stress. Therefore, to simplify the design problem, it is assumed that the support diameter is determined firstly, and then the depth and location are decided in a subsequent step.

Considering available tool sizes for drilling, we restricted support diameters to equal multiples of 1/16 inch. The selection of the sacrificial support size is based on the worst-case stress scenario, where we assume only one support is available, and then when two can be placed, we have a safety factor in place. In a simple model of the conditions, we consider the stock to be a simple cylinder, and the diameter of the cylinder is computed from the minimum diameter of a cylinder that can enclose the bone cut section along the axis. The cutting force is calculated from the power requirement of the cutting tool generated by the material removal rate (MRR) and the unit horsepower [34, 35]. The approximated cutting force for aluminum and steel varies from 2 to 4.5 lbs [27]. Steel has a tensile strength range from around 300 MPa, up to more than 1882 MPa, depending on the type of alloy [36]. Bone on the other hand, has an ultimate strength of only around 298 MPa at most (From equation 5). Hence, the hardest cortical bone is still easier to machine than steel. For a conservative estimate of average cutting force for CNC-RP<sub>bio</sub>, a cutting force of 5 lbs is used for the worse-scenario analysis in this research. Table 1 shows the VonMises stress of the contact surface between the support (screw end) and the part. Our simulation results show the VonMises stress dramatically increases when the support diameter decreases from 1/8 inch to 1/16 inch. However, the ultimate compressive strength for the bone (cortical bone) is around 298 MPa (calculated from equation 5) which is less than the stress showing in Table 1 when the support size is chosen to be 1/16 inch. Considering the size of expected clinical bone implant (the minimal diameter of a cylinder that can enclose the implant would be around 1~1.5 inch), 1/4 inch support diameter would result in a large amount of implant surface becoming non-machinable, and large holes left after removing supports.

Therefore, 1/8 inch is chosen to be a suitable support diameter based on both the consideration of bone compressive strength and implant size [37].

Table 1. FEA results with different support depth and diameter for the cylinder with 2 inch length and 2.5 inch diameter (FEA unit MPa)

Depth h (in.)	0	0.2	0.4	0.6	0.8	1.0	1.2
<b>Diameter (in.)</b>							
<b>1/16</b>	587.9	559.4	578.0	509.6	591.5	602.3	570.8
	570.7	544.9	576.5	488.3	569.6	601.2	573.0
	570.6	557.1	556.9	502.2	559.8	628.0	551.0
	585.3	564.8	557.9	517.3	589.1	619.7	570.9
<b>1/8</b>	72.72	68.41	59.33	59.37	61.34	71.49	63.29
	73.56	67.45	63.36	63.75	62.11	73.60	64.95
	73.46	66.59	64.36	66.30	64.94	72.04	67.61
	70.18	67.07	61.29	62.41	64.51	66.64	62.14
<b>1/4</b>	7.134	7.894	6.627	7.886	7.767	8.040	8.113
	7.318	7.769	7.391	7.979	7.670	7.593	8.882
	7.364	7.413	7.674	8.109	7.654	8.031	7.825
	7.578	7.293	7.028	8.741	7.440	7.801	7.602

### ***Location of sacrificial support***

The first step for determining locations for the screws are to calculate the diameter of the cylinder that can enclose the cut bone section. According to that diameter, a stress prediction function is chosen to estimate the VonMises stress. The second step is to offset the slice contour of the part model inwardly or outwardly by more than the radius of the screw. Recall that the *Matryoshka* shell model divides the 3D volume of the bone into different regions, bounded by different shells. For the shells between the cancellous and outer surface, the slice contours of the shells are offset outwardly by more than the radius of the support radius. Then, a shell is selected to provide minimal thresholding

bone density value, and the location of the supports can only lie in the region where the bone density is above the threshold value.

Figure 9 demonstrate the examples when different shells are selected to provide a minimal HU thresholding value to enforce that support locations should be embedded into specific regions and the corresponding support depth should be minimized accordingly. In Figure 9(a), a medullary cavity shell (shell 1) is chosen as the boundary so that two supports generated on the right side are slightly inserted into the bone implant surface and embedded into the low-density cancellous bone region. In this scenario, support depth  $d_1=d_2 = 0.2$  inch. If a low-cancellous bone shell (shell 2) is selected to be the boundary, the support will pass through the entire low-density cancellous bone region and terminate in the high-density cancellous bone region, as shown in Figure 9(b). To minimize the support depth, the depth of the screw penetration into the high-density cancellous bone region is 0.2 inch.

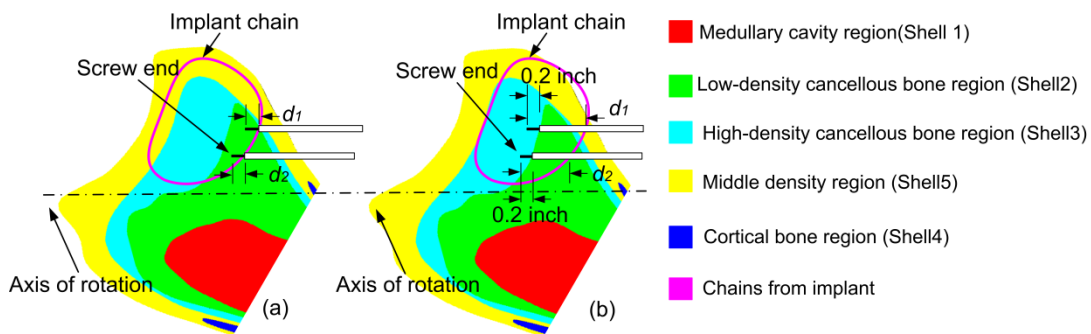


Figure 9. Examples to minimize the support depth when different shells are selected to be the HU thresholding boundary. (a) Medullary cavity shell (shell 1) chosen; (b) Low density cancellous shell (shell 2) chosen.

To estimate the VonMises stress in the implant, we first assume the bone cut stock is approximated as a cylinder, as shown in Figure 10(b). The radius of the cylinder is calculated from the minimum radius cylinder that could contain the part. The support locations within the cylinder can be represented by the coordinates  $(x_1, y_1, z_1)$  and  $(x_2, y_2, z_2)$ . We also assume the worst scenario that on one side of the cylinder stock there is only one support located at the center of cylinder surface, and on the other side of the cylinder two supports can be placed, shown in Figure 10(b). Since a cylinder is a symmetric object about its center axis, the representation of the support location within the cylinder can be simplified by five parameters. They are: the depths of supports 1 ( $h_1$ ) and 2 ( $h_2$ ) within the stock, the distance between the center of support 1 and support 2 ( $D$ ), the distance between the center of the support 1 to the center of rotation axis ( $l_1$ ), and the distance between the center of the support 2 to the center of rotation axis ( $l_2$ ), as shown in Figure 10(b) and (c). The function to estimate the VonMises stress is expressed in the implicit function (9).

$$\text{Stress} = \text{Func}(l_1, l_2, D, h_1, h_2) \quad (9)$$

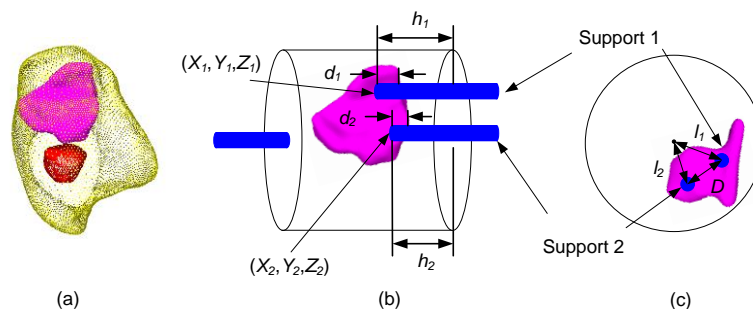


Figure 10. Support layout. (a) Implant within bone cut stock; (b) Implant within cylinder stock; (c) Cross section view of the stock.

To predicate the coefficients in the implicit function (9), a regression method is used to estimate the VonMises stress of different combinations of  $l_1, l_2, D, h_1, h_2$  for a two-support layout from Finite Element Analysis (FEA). Two different regression methods, Kriging approximation and multiple curvilinear regression methods are compared, in order to better predict VonMises stress from the five variables.

Kriging is a method of interpolation that was originally developed in geostatistics by a South African mining engineer [38]. The Kriging model has been used in a wide variety of fields, including geological mapping, meteorology, climatology, and mechanical engineering. It is also used to approximate the response of computer experiments, especially when optimization problems require expensive simulations using finite element methods (FEA) or computational fluid dynamics (CFD) [39].

The basic idea of Kriging is to predict the value of a function at a given point by computing a weighted average of the known values of the function in the neighborhood of the point. In order to construct a Kriging model, a spatial correlation function has to be chosen. The correlation function could be Exponential, Gaussian, Linear, Cubic, Spline or a Spherical function; depending on the property of physical model used. The Gaussian function is the most commonly used in engineering design as it provides a continuously differentiable surface, making it useful with gradient-based optimization algorithm [40].

The mathematical form of a Kriging model has two parts, as shown in Equation (10).

$$y(x) = f(x) + Z(x) \quad (10)$$

The first part is a deterministic contribution function  $f(x)$ , which is usually represented by a low order polynomial. The second part is a stochastic component  $Z(x)$ , which is a model of a Gaussian and stationary random process with zero mean and covariance:

$$\text{Cov}[Z(x^i), Z(x^j)] = \sigma^2 \mathfrak{R}(R(x^i, x^j)) \quad (11)$$

Where  $\sigma^2$  is the process variance,  $\mathfrak{R}$  is the correlation matrix and  $R(x^i, x^j)$  is the correlation function between data points  $x^i$  and  $x^j$ . We assume the VonMises stress prediction function (9) is continuously differentiable, and a Gaussian function is chosen as a correlation function. In this case,  $R$  is given by:

$$R(x^i, x^j) = \prod_{k=1}^m e^{-\theta_k |x_k^i - x_k^j|^2} \quad (12)$$

Figure 11(a) shows the residual plot using Kriging approximation for a given stock cylinder of 2.5 inch diameter and 2.5 inch length. In this case, 231 data points are random generated for analysis. The mean value and standard deviation of the residuals are -0.13 MPa and 2.49 MPa, respectively. From Figure 11(a), one can see that the residual varies from -9.93 MPa to 8.15 MPa. Figure 11(b) demonstrates the corresponding residual plot using a multiple curvilinear regression method. The mean value and standard deviation of the regression is  $-1.91e^{-011}$  MPa and 1.33 MPa, respectively. The range of residual is from -3.63 MPa to 4.09 MPa, which is less than the result from Kriging approximation method. Compared the residual plot from Kriging approximation and multiple curvilinear regression method, the latter one has less

residual value, which indicates the multiple curvilinear regression general gives a better VonMises stress prediction then the Kriging approximation method in this case.

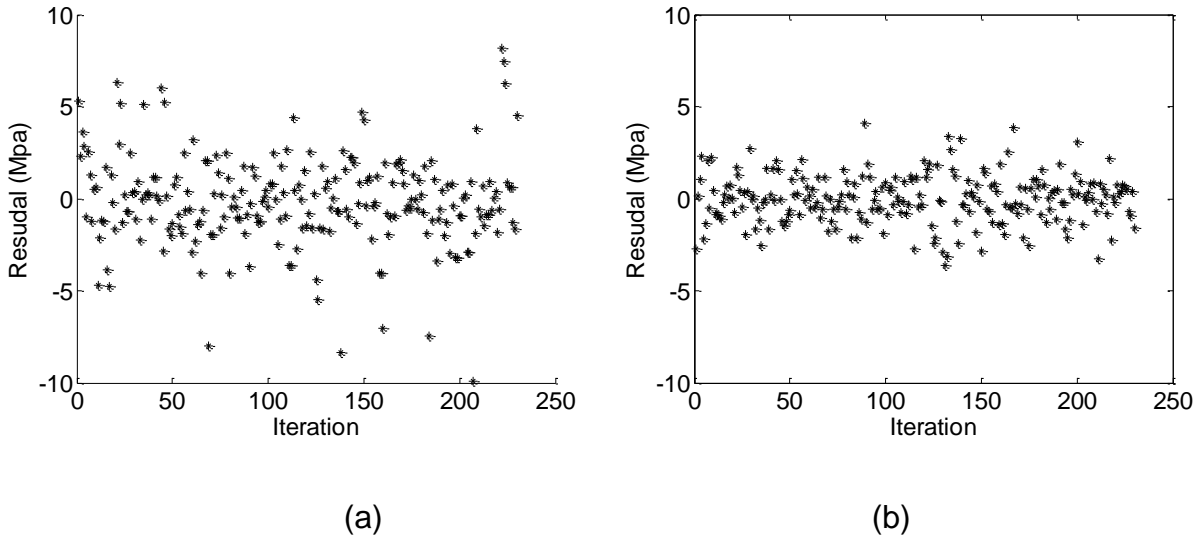


Figure 11. Residual plot from Kriging approximation method and multiple curvilinear regression method. (a) Kriging approximation: Mean = -0.13 MPa, std deviation = 2.49 MPa; (b) Multiple curvilinear regression; Mean =  $-1.91e^{-011}$  MPa, std deviation = 1.33 MPa.

Table 2 shows the regression analysis result when different orders of polynomial functions are used. An RSquare value closer to 1 indicates a better fit to the data and a smaller residual indicates a model is a much better predictor of the data. From the data shown in Table 2, a fourth degree polynomial function is a better fit function than other lower degree polynomial functions.

Table 2. Regression analysis for different orders of polynomial functions

Function degree	Summary of Fit			Residual Analysis	
	RSquare	RSquare Adj	Root Mean Square Error	Mean	Std Deviation
Quadratic	0.9327	0.9263	2.5666	0	2.4519
Cubic	0.9761	0.9689	1.6678	0	1.4621
Fourth degree	0.9802	0.9735	1.5398	0	1.3306

Based on the multiple curvilinear regression method, a 4-degree polynomial function is proposed to predict the VonMises stress. For one setup rotation, there might be more than one pair of supports locations available on each end. One example is shown in Figure 12(a), which demonstrates there are four locations available for add the sacrificial supports. After applying the criteria that the VonMises stress should be less than the 50% of ultimate stress of the material, the number of available support locations is reduced to three, shown in Figure 12(b). According to the constraint that the center of the pair of supports should be at least twice of  $D_t + 2r$ , support  $r_2$  is excluded from the layout and the final support location is  $r_1$  and  $r_3$  shown in Figure 12(c). In general, the objective function of the support design is:

Objective Function: Minimize support depth ( $\sum d_i$ ).

Constraint 1: VonMises stress  $< 0.5(\text{Compressive stress})$ .

Constraint 2: Distance between two supports  $> 2(D_t + 2r)$ .

Constraint 3: A shell is selected to provide minimal thresholding bone density value, and the location of the supports can only lie in the region where the bone density is above the threshold value.

Constraint 4: Maximize the distance between two supports.

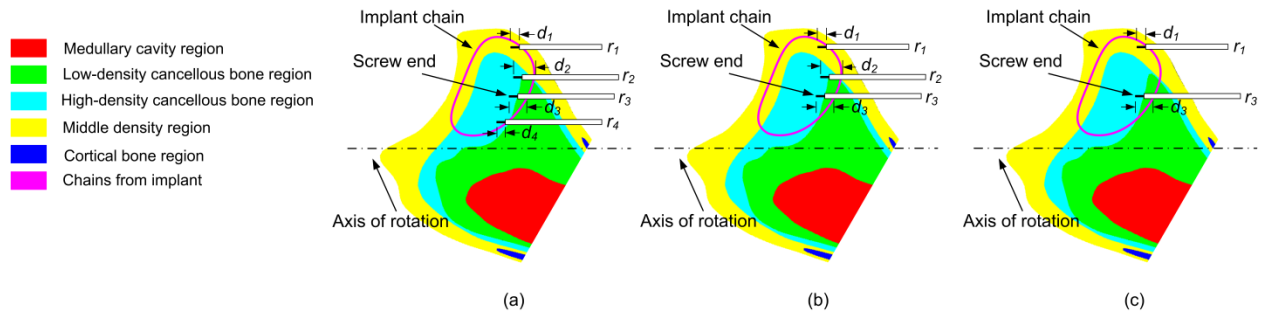


Figure 12. Illustration of step to select the final sacrificial support layout.

#### 4.4 Implementation Example

##### ***Matryoshka* Model generation**

The HUs used to generate the *Matryoshka* shell model can be determined by the following procedures. We firstly assume a worse-scenario where only one support on each side is possible; the support layout is 1:1. FEA is used to predict the VonMises stress from the stock for a 1:1 support layout. The stock is approximated as a cylinder, and the diameter of the stock varies from 1.5 inch to 2.5 inch and the length of the cylinder ranges from 1.5 inch to 2.5 inch. The supports are located at the center of the cylinder surface and embedded into the cylinder with different depth. The VonMises stress from the FEA result ranges from 37.6 MPa to 73.56 MPa. The HU value obtained after applying the equation (5) and (6) ranges from 531 to 744. For this scenario, if the support layout is 1:1, the bone region that supports can be embedded into should have HU value above 531 at least.

The other scenario is to assume two supports can be located on each side; the support layout is 2:2. The supports are located far apart and are generally centered about the

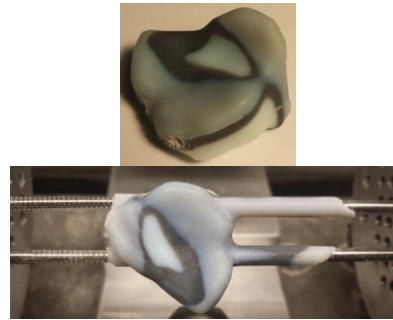
axis of rotation from the part in process, and the supports are embedded into the cylinder stock with different depth. The VonMises stress from the FEA result varies from 9.58 MPa to 16.44 MPa. After applying the equation (5) and (6), the HU value ranges from 268 to 351. These two HU values indicate that if two supports are embedded into the bone region, the HU value of that region should be at least 268.

In this implementation, HU values from 210 and 850 are used to generate a canal shell and cortical bone shell for a given set of CT data. An HU value of 550 is used to create another shell for a worse-scenario; wherein, if only one support on each side is possible, then the support end can only be in the region outside of this shell. Conversely, if two supports can be placed on each end, it is better that the support ends should go to the bone region where the HU value is greater than 350. In summary, the HU values used to generate *Matryoshka* shell models in this work are: 210, 350, 550, and 850.

The algorithms developed in this work have been implemented in C++ within a MasterCam CAD/CAM software add-on being developed - CNC-RP<sub>bio</sub>. Several bone implant models have machined using the developed support design algorithms, as illustrated in Figure 12. In order to mimic the multiple density shell regions of the prototype bone surrogate, an Objet Connex 3D printer was used to additively manufacture a multiple color plastic *Matryoshka* shell model of a human tibia (Figure 13 (a) and (b)).

The implant models shown in Figure 13 have a length of 1.14 in, width of 0.78 in, and the thickness of 0.95 in. Figure 14(b) shows the assembled *Matryoshka* Model with the harvested implant. Shell1 is selected as a boundary so that the supports can only lie in the region between shell1 and outer surface. The compressive stress is set to be 50 MPa. The process planning starts with slicing the *Matryoshka* model and implant at 1.0 mm spacing. Each support is approximated as a cylinder and the support diameter is chosen to be 1/8 inch.

Implant size: 1.14 x 0.78 x 0.95 inch  
 Support diameter: 1/8 inch  
 Left support location  
 Support 1: x: -1.49, y: 0.20, z: 0, depth  $d_1$ : 0.24  
 Support 2: x: -1.34, y: 0, z: -0.40, depth  $d_2$ : 0.24  
 Right support location  
 Support 3: x: -1.22, y: 0, z: 0, depth  $d_3$ : 0.28  
 Support 4: x: -1.26, y: 0, z: -0.40, depth  $d_4$ : 0.31  
 (a)



Implant size: 1.14 x 0.78 x 0.95 inch  
 Support diameter: 1/8 inch  
 Left support location  
 Support 3: x: -1.17, y: 0, z: 0, depth  $d_3$ : 0.51  
 Support 4: x: -1.17, y: 0, z: -0.40, depth  $d_4$ : 0.51  
 Right support location  
 Support 1: x: -1.20, y: 0, z: 0, depth  $d_1$ : 0.24  
 Support 2: x: -1.32, y: 0, z: -0.40, depth  $d_2$ : 0.24  
 (b)



Figure 13. Implementation examples using designed sacrificial supports in the machining process.

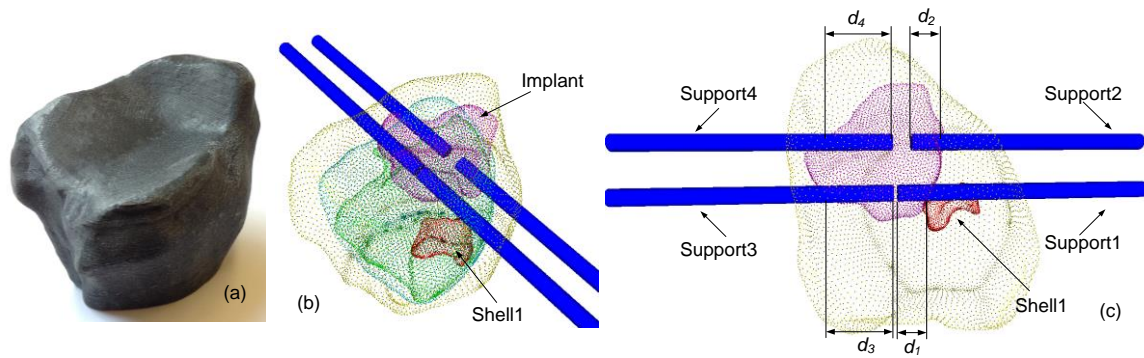


Figure 14. Support design

The process planning steps, including sacrificial supports, are automatically generated within the MasterCam software add-on CNC-RP<sub>bio</sub>. Bone cut section rotations, translations, drill support locations, depths, etc. are provided in a setup sheet from the software. This setup sheet provides the detailed instructions required for machinists to properly embed surgical screws into the bone. The machining tool paths for the bone implant are generated based on the existing methods developed for CNC-RP<sub>bio</sub>, using MasterCAM toolpath functions commanded by the add-on.

To evaluate the effectiveness of the support design method, the machined bone implant was scanned to compare the different color surface areas between the initial implant CAD model and the scanned model. The underlying assumption is that if the support screw location was good, then one should expect the final implant to have the same density distributions as originally planned; else, the bone shifted, bent or otherwise moved under cutting conditions. The scanned implant model was imported into Geomagic RapidForm software to create bounding lines for different color surface regions. Figure 15 provides an example of a scanned color bone implant and Table 3

provides the surface area comparison results between the initial implant CAD model and the resulting 3D scanned model. As can be seen, the area difference for different color surface region is very small, which indicates the fixture system provides a robust and accurate support location.

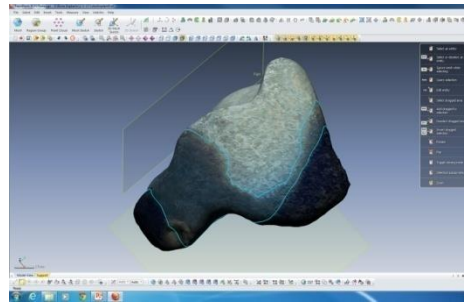


Figure 15. An example of 3D scan of color bone implant.

Table 3. Surface area comparison between initial implant CAD model and 3D scanned model (Unit mm<sup>2</sup>).

Surface	Initial CAD model	Scanned model	Difference	% Difference
White	630	578	52	8.3%
Grey	337	329	8	2.4%
Black	628	745	117	18.6%
<b>Total</b>	1595	1652	57	3.6%

Next, the CAD model of machined implant with the support design was imported to Abaqus to simulate the stress of the contact surface between the implant and embedded screws. An example of the implant and supports CAD model is shown in Figure 16. In this simulation, the largest expected cutting force is applied, and the cutting force is applied tangentially through four different directions. Table 4 provides the FEA result of predicted VonMises stress. From the result shown in table 4, the

maximal stress is 19.27 MPa, occurring at the contact surface between support 3 and bone implant; which is less than the compressive strength of 50 MPa in the implementation example.

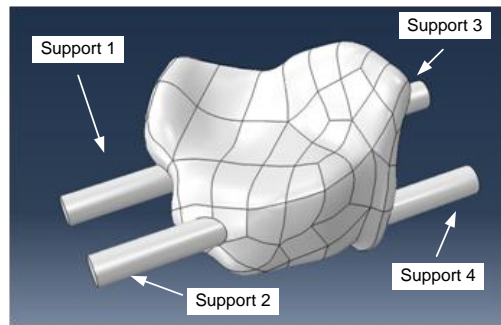


Figure 16. CAD model of the implant with support design.

Table 4. FEA result of CAD model of the implant with support design (Unit MPa)

	Support1	Support2	Support3	Support4
0 degree	0.97	6.74	1.89	19.00
90 degree	5.36	14.44	9.68	9.91
180 degree	7.34	6.81	19.27	3.63
270 degree	6.52	14.63	8.29	7.69

#### 4.5 Conclusion

This paper presents a method for creating sacrificial support fixtures for the subtractive rapid machining process of heterogeneous materials, namely, automated bone implant manufacturing. The approach of fixture design has been shown to work well for several surrogate bone implants machined in the laboratory. Compared with the traditional hand-sculpting of bone implant by surgeons, this method provides the potential to completely automate the process, and, should greatly improve the geometric accuracy of the implants. The expectation is that a more accurate bone implant geometry will

yield better initial fixation stability and better overall outcomes. This includes better alignment of the joints post-surgery, which can lead to reductions in osteoarthritis years later. Being completely automated process planning should also make the process affordable, even in the presence of custom fits for each and every new patient versus mass production.

However, this approach still leaves room for improvement and refinement. In general, the proposed solutions are largely predicated on the assumption of a general case of sizes of implants and available surgical tools, it is not very generic. Future research could analyze the parameters which can affect the stress generated by support insertion process, using a much more general classification of screws and drills. Whereas the resulting configuration suggests ~1/8 surgical screw, this is by no means an optimal size for all implants in all cases. Work would need to consider a broader range, and show how a continuous spectrum of design parameters, not just a discrete set of available off-the-shelf surgical tools and fixators could be used. In order to evaluate the effectiveness of the support design method, future work could measure the machined part to analyze cracks, and estimate stress within the part, in addition to the surface geometry comparison.

#### **4.6 Reference**

[1] Pehlivan, S. and Summers, J.D., A review of computer-aided fixture design with respect to information support requirements, *International Journal of Production Research*, 2008, 46(4), 929-947.

- [2] Bi, Z. M. and Zhang, W.J., Flexible fixture design and automation: Review, issues and future direction, *International Journal of Production Research*, 2001, 39(13), 2867-2894.
- [3] Chua, C.K., Leong, K.F., and Lim, C.S., *Rapid prototyping: principles and applications*, World Scientific, 2010.
- [4] Kruth ,J.P., Wang, X., Laoui ,T. and Froyen L., Lasers and materials in selective laser sintering, *Assembly Automation*, 2003, 23(4), 357-371.
- [5] Sachs, E., Wylonis, E., Allen, S., Cima, M. and Guo, H., Production of injection molding tooling with conformal cooling channels using the three dimensional printing process, *Polymer Engineering & Science*, 2000, 40(5), 1232-1247.
- [6] Huang, X., Ye, C., Wu, S., Guo, K. and Mo, J., Sloping wall structure support generation for fused deposition modeling, *The International Journal of Advanced Manufacturing Technology*, 2009, 42(11-12), 1074-1081.
- [7] Ziemian, C. W. and Crown III, P. M., Computer aided decision support for fused deposition modeling, *Rapid Prototyping Journal*, 2001, 7(3), 138-147.
- [8] Strano, G., Hao, L., Everson, R. M. and Evans, K. E., A new approach to the design and optimisation of support structures in additive manufacturing, *The International Journal of Advanced Manufacturing Technology*, 2013, 66(9-12), 1247-1254.
- [9] Giannatsis, J. and Dedoussis , V., Decision support tool for selecting fabrication parameters in stereolithography, *The International Journal of Advanced Manufacturing Technology*, 2007, 33(7-8), 706-718.
- [10] Sun, W., Multi-volume CAD modeling for heterogeneous object design and fabrication, *Journal of Computer Science and Technology*, 2000, 15(1), 27-36.
- [11] Chen, K. Z. and Feng, X. A., CAD modeling for the components made of multi heterogeneous materials and smart materials, *Computer-Aided Design*, 2004, 36(1), 51-63.
- [12]<http://www.stratasys.com/3d-printers/design-series/precision/objet-connex500> (accessed April 3<sup>rd</sup> 2013).
- [13] Hague, R., Mansour, S. and Saleh, N., Material and design considerations for rapid manufacturing, *International Journal of Production Research*, 2004, 42(22), 4691-4708.
- [14] Hao, L., New material development for laser additive manufacturing, *Proceedings of the 5th International Conference on Advanced Research in Virtual and Rapid Prototyping*, 2011, 359-364.

- [15] Frank, M.C., Wysk, R. A. and Joshi, S. B., Rapid planning for CNC milling - a new approach for rapid prototyping, *Journal of Manufacturing Systems*, 2004, 23(3), 242-255.
- [16] Frank, M.C., Hunt, C.V., Anderson, D.D, Mckinley, T.O. and Brown, T.D., Rapid manufacturing in biomedical materials: using subtractive rapid prototyping for bone replacement, Proceedings of the Solid Freeform Fabrication Symposium, 2008, 686-696.
- [17] <http://academic.uofs.edu/faculty/kosmahle1/courses/pt245/trabecul.htm> (accessed October 20<sup>th</sup> 2012).
- [18] Kang, X and Peng, Q., Fixture feasibility: methods and techniques for fixture planning, *Computer Aided Design and Applications*, 2008, 5(1-4), 424-433.
- [19] Joneja, A and Chang, T.C., Setup and fixture planning in automated process planning systems, *IIE Transactions*, 1999, 31(7), 653-665.
- [20] Tseng, Y.J., Fixturing design analysis for successive feature-based machining, *Computers in Industry*, 1999, 38(3), 249-262.
- [21] Gandhi, M.V. and Thompson, B.S., Phase change fixturing for flexible manufacturing systems, *Journal of Manufacturing Systems*, 1985, 4(1), 29-39.
- [22] Gandhi, M.V., Thompson, B.S. and Maas, D.J., Adaptable fixture design: an analytical and experimental study of fluidized-bed fixturing, *Journal of Mechanisms Transmissions and Automation in Design*, 1986, 108(1), 15-21.
- [23] Choi D.S., Lee S.H., Shin B.S., Whang K.H., Yoon K.K. and Sarma, S.E., A new rapid prototyping system using universal automated fixturing with feature-based CAD/CAM, *Journal of Materials Processing Technology*, 2001, 113(1), 285-290.
- [24] Shin, B.S, Yang, D.Y., Choi, D.S., Lee, E.S. Je, T.J. and Whang, K.H., A new rapid manufacturing process for multi-face high-speed machining, *The International Journal of Advanced Manufacturing Technology*, 2003, 22(1-2),68-74.
- [25] <http://www.deskproto.com/support/videos-venus.htm> (accessed April 3<sup>rd</sup> 2013).
- [26] <http://www.rolanddga.com/products/milling/mdx540/#overview> (accessed April 3<sup>rd</sup> 2013).
- [27] Boonsuk, W and Frank, M.C., Automated fixture design for a rapid machining process, *Rapid Prototyping Journal*, 2009, 15(2), 111-125.

- [28] Chen, Y., A Contour-based Support Generation Method for Solid Freeform Fabrication of Complex Parts. *Proceedings of the Solid Freeform Fabrication Symposium*, 2009.
- [29] <http://digfablab.wikispaces.com/Envisiontec+Perfactory+RP> (accessed April 3<sup>rd</sup> 2013).
- [30] Lei, S., Frank, M.C., Anderson, D.D, and Brown, T.D. A method to represent heterogeneous materials for rapid prototyping – the Matryoshka approach. *Rapid Prototyping Journal*, 2014, 20(5), Accepted.
- [31] Biewener, A.A., Safety factors in bone strength. *Calcif Tissue Int*, 1993,53(1),68-74.
- [32] Frost, H. M., On the strength-safety factor (SSF) for load-bearing skeletal organs, *J Musculoskelet Neuronal Interact*, 2003, 3(2), 136-140.
- [33] Carter, D.R. and Hayes, W.C. Bone compressive strength: the influence of density and strain rate. *Science*, 1976, 194(4270), 1164-1176.
- [34] Scheider, R., “Start with the right speeds and feeds”, MMS online, available at: <http://www.mmsonline.com/articles/start-with-the-right-speeds-and-feeds> (accessed Jan 20<sup>th</sup> 2013).
- [35] Spitzler, D., Lantrip, J., Nee, J.G. and Smith, D.A., Fundamentals of tool design, Society of Manufacturing Engineers, 2003.
- [36] [http://www.efunda.com/materials/alloys/alloy\\_home/steels\\_properties.cfm](http://www.efunda.com/materials/alloys/alloy_home/steels_properties.cfm)(accessed June 30<sup>th</sup> 2014).
- [37] Farmanullah, K. M. and Awais , S. M., Evaluation of management of tibial non-union defect with Ilizarov fixator, *J Ayub Med Coll Abbottabad* ,2007, 19(3), 35-36.
- [38] Krige D. A statistical approach to some basic mine valuation problems on the Witwatersrand. *Journal of the Chemical, Metallurgical and Mining Society of South Africa*, 1951, 52, 119-139.
- [39] Kok, S., The asymptotic behaviour of the maximum likelihood function of kriging approximations using the Gaussian correlation function. EngOpt 2012 - International Conference on Engineering Optimization, Anonymous Rio de Janeiro, 2012.
- [40] Martin, J. D. and Simpson, T. W., On the use of kriging models to approximate deterministic computer models. In ASME 2004 International Design Engineering Technical Conferences and Computers and Information in Engineering Conference, 2004.

## CHAPTER 5: CONCLUSION AND FUTURE WORK

The chapter summarizes this dissertation and provides some ideas for future work.

### 5.1 Summary

This dissertation proposed a subtractive rapid manufacturing process for heterogeneous materials, in particular for custom shaped bone implants. This includes two major areas of research that will enable automated process planning of this new process. The methodologies proposed in this dissertation have been implemented in a process planning software, called CNC-RP<sub>bio</sub>. Several bone implants have been machined using this software, and the results show the methodologies provide an effective and robust process planning for the rapid manufacturing of bone implants from natural bone.

Firstly, a new method for multi-material model representation using nested polygonal shells, called the *Matryoshka* shell model, was presented. This model is based on the varying density distribution of human bone. The *Matryoshka* model is generated via an iterative process of thresholding the Hounsfield Unit (HU) data from a computed tomography (CT) scan, thereby delineating regions of progressively increasing bone density. The method of choosing a suitable number of shells and the thresholding HU value for generating each shell were also illustrated. Compared with the method of hand-creating an assembly model for input to a multi-material additive RP system, this method could potentially be completely automated from a given set of parameters.

Next, a harvesting algorithm was proposed, which could determine a suitable location for the bone implant from within natural bone based on the *Matryoshka* model. In this harvesting algorithm, a density score and similarity score are calculated to evaluate the overall effectiveness of that harvest site. An interactive graphics program has been developed based on this harvest algorithm. The software allows the user to move the implant CAD model within the bone design space and observe the density score and similarity score of the implant at candidate harvesting locations. The benefits of this software would be most helpful from the clinical perspective. The surgeon can use this software to choose a best fit for both geometry and density. However, the *Matryoshka* shell model is not a generic solution for all multi-material components; it is most effective for human long bones. If the desired donor bone is not a long bone, future work with the *Matryoshka* approach would need to develop a better harvesting solution for irregular and/or flat bones.

The second research area was to develop an automated fixturing system for securing the bone implant during the machining process. During the machining process, the material around the embedded sacrificial supports are machined, and at the end of the process, only the supports are connected to the part and the remaining designed fixture disks. The proposed method uses a variant of sacrificial supports (stainless surgical screws, etc.) to pass in appropriate orientations through the free-form shaped stock, terminating at proper locations inside the solid part model of the implant. The parameters required for this design are the depth, diameter, and location of the sacrificial supports, and are dependent on the density distribution of the part material.

Based on these design parameters, an objective function, which minimizes the imbedded support depth with certain constraints, was proposed to determine the optimal location of the supports termination inside the bone implant. This automated fixturing system has been applied to machine several bone implants made of assembled colored-RP models, where the final machined implants show the designed fixturing system successfully provides stiffness to the part to enable accurate machining.

Finally, the algorithms that were developed for setup planning are implemented in a CAD/CAM software add-on called "CNC-RP<sub>bio</sub>". This software can automatically determine process planning parameters, such as choosing the optimal rotation axis of the CAD model and creating the sacrificial support structures on each end of the CAD model automatically. Several complex implant parts were machined using this software. The result shows this software can be used as an automated process planning tool for the rapid machining of custom shaped bone implants, which could create unique implants at the touch of a button.

One future direction would be to improve the harvest search algorithm to find the optimal implant harvest site for irregular and/or flat bones. Another future work should explore utilizing the *Matryoshka* model and automated fixturing design to determine a suitable axis of rotation for automated rapid machining of natural bone implants.

## 5.2 Future Work

### 5.2.1 Improving the Harvest Search Algorithm

The approach presented in this research to find the optimal implant harvest site within a donor bone is not necessarily a generic solution for all natural bones. It is intended for human long bones, since long bones can be approximated as a cylinder model and it is relatively easy to find the center line of the bone (Figure 1(a) and (b)). In addition, a long bone generally exhibits increasing density as one moves away from the bone center line radially (Figure 1(c)). A proposed harvest search approach would be to find the gradient direction that corresponds to bone density increase for irregular and/or flat bones bones, and then by comparing or matching the density gradient direction of the donor bone and the implant, an optimal implant harvest site location could be obtained.

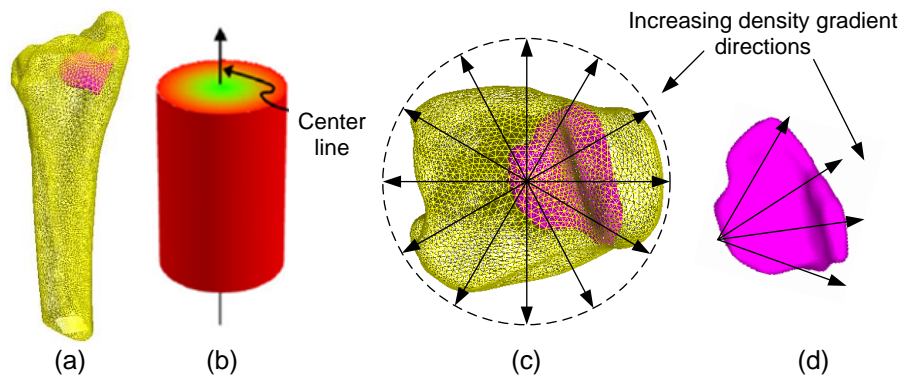


Figure 1. Illustration of harvesting an implant from a donor bone. (a) A selected harvest location within the donor bone; (b) A cylinder approximation of donor bone; (c) increasing density gradient directions for the donor bone (c) and the implant (d).

### 5.2.2 Rotation Axis Selection

In this dissertation, we have presented two major areas of research what will enable automated process planning for a rapid manufacturing of heterogeneous materials, applied to natural bone implant manufacturing. The areas are using the *Matryoshka* shell model to represent the heterogeneous material and the automated fixture design methods. However, a rotation axis needs to be determined before applying the fixture design.

An algorithm that can determine a suitable rotation axis for bone implant machining can be developed based on the results from *Matryoshka* shell model and fixture design. Some of the factors that are included in this algorithm could be the percentage of visibility of the implant model, feasible locations for the sacrificial supports, and the non-machinable region blocked by the imbedded sacrificial supports.

#### ***Discretization of a sphere***

A proposed first step might be to discretize the unit sphere into a grid of discrete points, as shown in Figure 2. The axes of rotation are represented to connect the center point *O* of the sphere with the discrete points on the sphere surface. The number of points on the sphere is:

$$\text{Num (points/axes)} = M \times N, \text{ where } M = \text{integer} \left( \frac{180}{a} \right) \text{ and } N = \text{integer} \left( \frac{180}{b} \right)$$

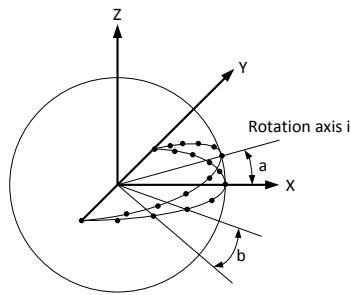


Figure 2. Discretization of a sphere

### ***Visibility calculation***

For each given rotation axis  $i$ , the visibility percent of the model would need to be calculated. For each segment on the slice model, one would check if the segment is visible or non-visible. The procedure to check the visibility can be classified into two steps: (1) checking the visibility of the segment with respect to other segments on the same chain and; (2) checking the visibility of the segment with respect to other segments on other chains but within the same slice. If both the result from the two steps gives the result that the segment is visible, we can define the segment is visible.

### ***Non-machinable region blocked by the imbedded sacrificial supports***

For each given rotation axis  $i$ , sacrificial supports are generated based on the fixture design approach presented in Chapter 4. However, the amount of non-machinable surface area depends on not only the increasing size of the support but also the geometry of the surface that the support is attached to. To illustrate this effect, an example of an implant with supports is demonstrated in Figure 3. The procedure to identify non-machinable region follows two steps: (1) identifying the implant chain

segments within the support chains and; (2) Identifying the non-visibility segments of the unioned chains between the implant chains and the support chains. The result from the two steps give the overall non-machinable region blocked by the embedded sacrificial supports.

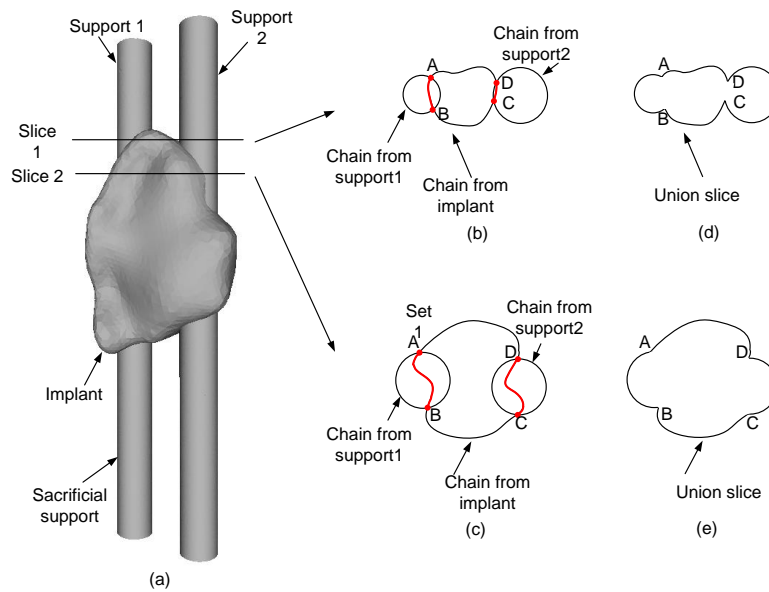


Figure 3. Support location and Non-machinable segment

Figure 3(a) shows an implant with the desired sacrificial supports. The cross sectional view of slices 1 and 2 are shown in Figure 3(b) and (c) respectively. The segments AB and CD highlighted in red are the non-machinable segment blocked by the embedded sacrificial supports, which will give the non-machinable analysis from step 1. Figures 3(d) and 2(e) illustrate the result after applying the union operation between implant slices and support slices. The visibility analysis of the union slices will give the non-machinable analysis from step 2.

### ***Determination of the optimal rotation axis***

The determination of the optimal rotation axis depends on three factors: the visibility percentage of the model, non-machinable percentage of the model caused by the embedded sacrificial supports, and the possibility of adding a sacrificial support for the rotation axis. A score could be used to describe the third factor quantitatively. Finally, an optimal function which considers all three factors is proposed to evaluate the “goodness” of each rotation axis.

Final score =  $\alpha \times$  visibility percentage +  $\beta \times (1 - \text{non machinable percentage}) + \lambda \times$  support score.

The set of future work proposed in this section would take the next major step toward a nearly automated solution, from CT scan to final bone implant for surgery. Automatically generation the axis orientation for the implant could better define machinable solutions that are more optimized for other parameters. Given the highly traumatic cases involved with these implants, the time period is a matter of days between CT scans and the final surgery; hence, more automation would be very advantageous for sure. In closure, the methods of this dissertation will take us one large step forward in the ability to make custom implants at the push of a button and more importantly, to ultimately improve the outcome for patients suffering such terrible injuries.

## **ACKNOWLEDGEMENTS**

I would like to take this opportunity to express my gratitude and thanks to those who helped me with various aspects of conducting research and writing this thesis. This dissertation would not have been accomplished without their support.

First and foremost, I would like to express my deepest gratitude to my advisor Dr. Frank. His professional knowledge guides me in all the time of research and writing of this thesis. His continuous support helped me with the challenges that arose during my study and research. His kindness makes my work a pleasant experience. I could not have imagined having a better advisor and mentor for my Ph.D study.

Next, I would like to express my sincere gratitude to my committee members Dr. Winer, Dr. Peters, Dr. Jackman, and Dr. Rivero. I appreciate the great suggestion they gave for the accomplishment of this dissertation.

Next, I thank Ashish Joshi, Niechen Chen, Guangyu Hou, Joshua Adams in the Rapid Manufacturing and Prototyping Laboratory, for their help to me.

Last but not least, I owe the success of this thesis to my family for their love and support. I realize how lucky I am to have such great parents who give me the best they have for my life.